EMERALDS FROM THE KAFUBU AREA, ZAMBIA

J. C. (Hanco) Zwaan, Antonín V. Seifert, Stanislav Vrána, Brendan M. Laurs, Björn Anckar, William B. (Skip) Simmons, Alexander U. Falster, Wim J. Lustenhouwer, Sam Muhlmeister, John I. Koivula, and Héja Garcia-Guillerminet

Zambia is considered the world's second most important source of emeralds by value (after Colombia). The deposits are located near the Kafubu River in the Ndola Rural Restricted Area. Emeralds have been known from this region since 1928, but significant commercial production began only in the 1970s. As of mid-2004, most of the emeralds were being mined from large open-pit operations at the Kagem, Grizzly, and Chantete concessions. Economic emerald mineralization is confined almost entirely to phlogopite reaction zones adjacent to Be-bearing quartz-tourmaline veins that metasomatically altered Cr-bearing metabasite host rocks. Nearly all of the rough is cut in India and Israel. Zambian emeralds have relatively high R.I. and S.G. values, with inclusions typically consisting of partially healed fissures, as well as actinolite, phlogopite, dravite, fluorapatite, magnetite, and hematite. They contain moderate amounts of Cr, Mg, and Na, moderate-to-high Fe contents, and relatively high Cs and Li. Although many features of Zambian emeralds are comparable to those from other commercially important localities, in many cases they may be separated by a combination of their physical properties, microscopic characteristics, and chemical composition.

Zambia is one of the world's most significant sources of fine-quality emerald and has been called the second most important producer by value after Colombia (see, e.g., Suwa, 1994; Giuliani et al., 1998). For years, the mines in the Kafubu area (near the Kafubu River in the Ndola Rural Restricted Area) have produced emeralds of uniform color and size, which supported the cutting of vast quantities of calibrated goods. In addition, relatively large, fine stones are occasionally found (see, e.g., figure 1).

Several articles have been published on Zambian emeralds, especially the geology of the Kafubu area, physical properties, and inclusions (see, e.g., Koivula, 1982; Graziani et al., 1983; Milisenda et al., 1999; Seifert et al., 2004c). The present article provides an overview on various aspects of these emeralds, and includes updated information on the geology of the area, mining and production, and gemological properties. Much of the historic and geologic information was obtained during several months of fieldwork in 2001 by two of the authors (AVS and SV), who studied all the major Zambian emerald deposits and several minor ones (Seifert et al., 2004b,c). In July-August 2004, these authors also examined a new emerald area in the Musakashi area of north-central Zambia (see box A). Other authors (JCZ in 1995 and BA since 2002) have visited the deposits, and in September 2004 BA collaborated with authors JCZ, BML, and WBS on visits to four mines (Chantete, Grizzly, Pirala, and Twampane). Subsequently, JCZ visited Ramat Gan, Israel, to learn more about the production and distribution of Zambian emeralds.

See end of article for About the Authors and Acknowledgments.
GEMS & GEMOLOGY, Vol. 41, No. 2, pp. 116–148.

Figure 1. Zambia has been an important source of emeralds since the 1980s. Much of the production is polished into beads, such as those in these strands (maximum bead diameter is 16.2 mm). Relatively large, fine-quality Zambian emeralds also are faceted, such as the center stone (10.42 ct) in this ring. Courtesy of Pioneer Gems, New York; photo © Harold & Erica Van Pelt.

HISTORY

According to Sliwa and Nguluwe (1984), beryl mineralization was first discovered in the Kafubu area (at a locality that later became known as the Miku mine) in 1928 by geologists working for the Rhodesia Congo Border Concession Co. Although initial investigations did not reveal good-quality gems, Rhokana Co. and Rio Tinto Mineral Search of Africa continued small-scale exploration work into the 1940s and '50s. In 1966, the claim was passed to Miku Enterprises Ltd., and in 1971 the rights to the Miku area were taken over by Mindeco Ltd., a government-owned company. The region was subsequently mapped and the Miku deposit verified by Zambia's Geological Survey Department (Hickman 1972, 1973).

During the 1970s, when local miners discovered several more deposits, the Kafubu area became a major producer of good-quality emeralds. Due to the significant economic potential and extensive illegal mining, the government established a restricted zone and forcibly removed the population of this sparsely inhabited area.

In 1980, a new government-controlled agency, the Reserved Minerals Corp., took over the major deposits and prospecting rights to the surrounding region (Sliwa and Nguluwe, 1984). Kagem Mining Ltd. (owned 55% by Reserved Minerals and 45% by Hagura, an Indian-Israeli corporation) was authorized to conduct exploration and mining in the Kafubu area. A privatization agreement was signed between Hagura and the Government of Zambia in May 2001, and the transfer of shares recently was completed by the government (Govind Gupta, pers. comm., 2005).

Outside the Kagem properties, which lie on the north side of the Kafubu River, the emerald area has been subdivided into nearly 500 prospecting plots. However, many of these claims were established without the benefit of a thorough geologic evaluation. Small-scale mining currently takes place on dozens of claims, whereas mechanized activity is mostly concentrated on the Kagem, Grizzly, Chantete, and Kamakanga properties.

LOCATION AND ACCESS

The emerald mines are located in the Kafubu area (also known as the Ndola Rural Restricted Area) of central Zambia, about 45 km southwest of the town of Kitwe (figure 2). This region lies in the southern part of an important copper mining area known as the Copperbelt (Coats et al., 2001). The emerald deposits are distributed over ~200 km^2 within 13°02′–13°11′S latitude and 28°03′–28°11′E longitude, on both sides of the Kafubu River.

From Kitwe, the Kafubu area is accessed by a 15 km paved road to Kalulushi, and then by 30 km of poorly maintained gravel road. The principal mining localities are reached by several dirt tracks, most of which remain passable throughout the year.

The Kafubu River, a western tributary of the Kafue River, drains the area together with small perennial streams. Except for the quartzite ridges in the southeast, there are no prominent topographic

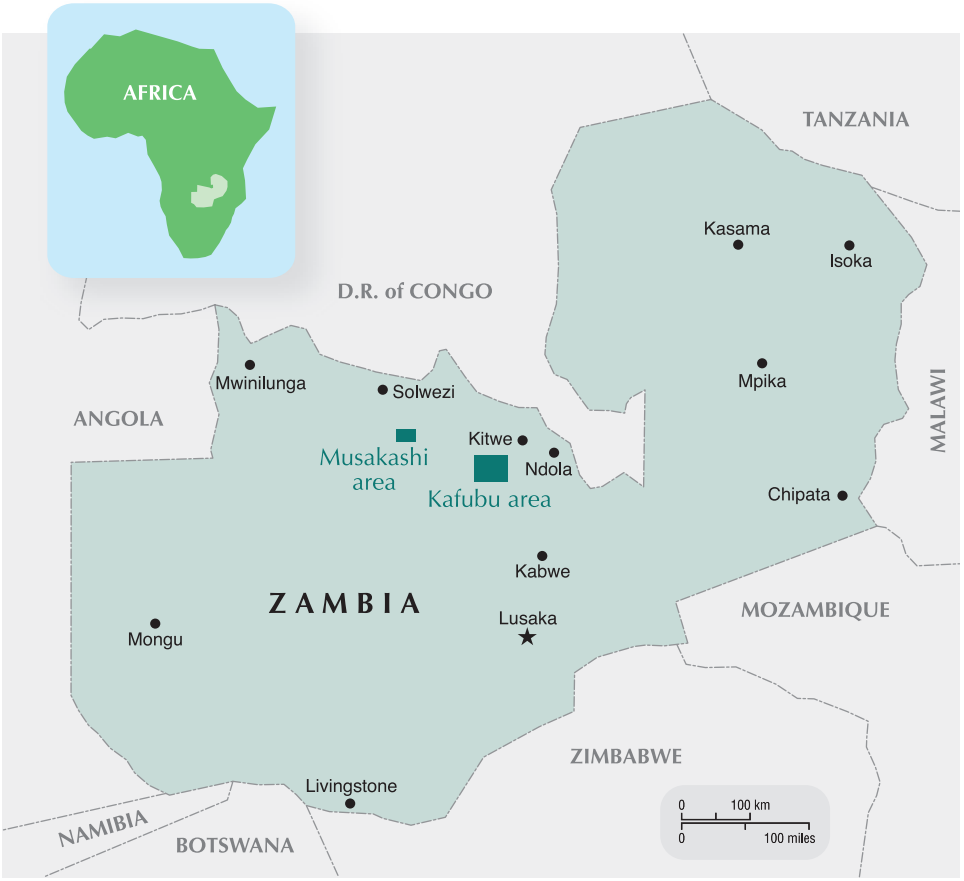

Figure 2. The Kafubu emerald mines are located in north-central Zambia, 45 km southwest of Kitwe, the nearest town. A relatively new emerald occurrence was discovered in the Musakashi area to the northwest of Kafubu in 2002.

features and the entire area is typically flat. The average altitude is around 1,200 m above sea level. Over much of the area, the residual clay-rich soils are yellow-brown or reddish brown with extensive crusts of laterite, and support relatively thick vegetation. Access to the area is restricted, although the workers' settlements are located near the producing mines.

GEOLOGY

Regional Geology. The region encompassing the Zambian Copperbelt and the Kafubu area comprises a complex assemblage of geologic units (figure 3) that evolved during three successive orogenies of mostly Proterozoic age (i.e., mountain-building events ranging from about 2 billion to 500 million years ago [My]). The emerald deposits are hosted by metamorphic rocks of the Muva Supergroup (Daly and Unrug, 1983) that overlay the basement granite gneisses along a structural unconformity. The Muva rocks consist of quartzites, mica schists, and metabasites. Emerald mineralization is hosted by the metabasites, which consist of talc-chlorite-actinolite ± magnetite schists (Hickman 1973; Sliwa and Nguluwe, 1984). These schists are thought to represent metamorphosed volcanic rocks that were dominated by komatiites (i.e., highly magnesian ultramafic rocks; Seifert et al., 2004c). Their high chromium content provides a necessary component for emerald mineralization.

In the Kafubu area, thick layers (up to 200 m) of the metabasite are intercalated in the mica schist–quartzite sequence. Deposition of the Muva Supergroup is dated to ~1,700 My. Subsequent folding and metamorphism, which also involved the basement granite gneisses, took place during the Irumide orogeny (~1,010 My; De Waele et al., 2002). Importantly, with the exception of the Kafubu area, the metabasites are unknown in other portions of the 1,000-km-long Irumide belt of northeastern Zambia (see, e.g., Daly and Unrug, 1983; De Waele and Mapani, 2002).

The basement granite gneisses and the Muva Supergroup were later buried under sediments of the Katanga Supergroup during the Neoproterozoic era (i.e., 570–900 My). The entire crustal domain then underwent folding, thrusting, and metamorphism during the Pan-African orogeny, culminating at ~530 My (John et al., 2004). This tectonic event produced the most observable deformation and metamorphic features in the Muva rocks of the Kafubu area (Hickman, 1973).

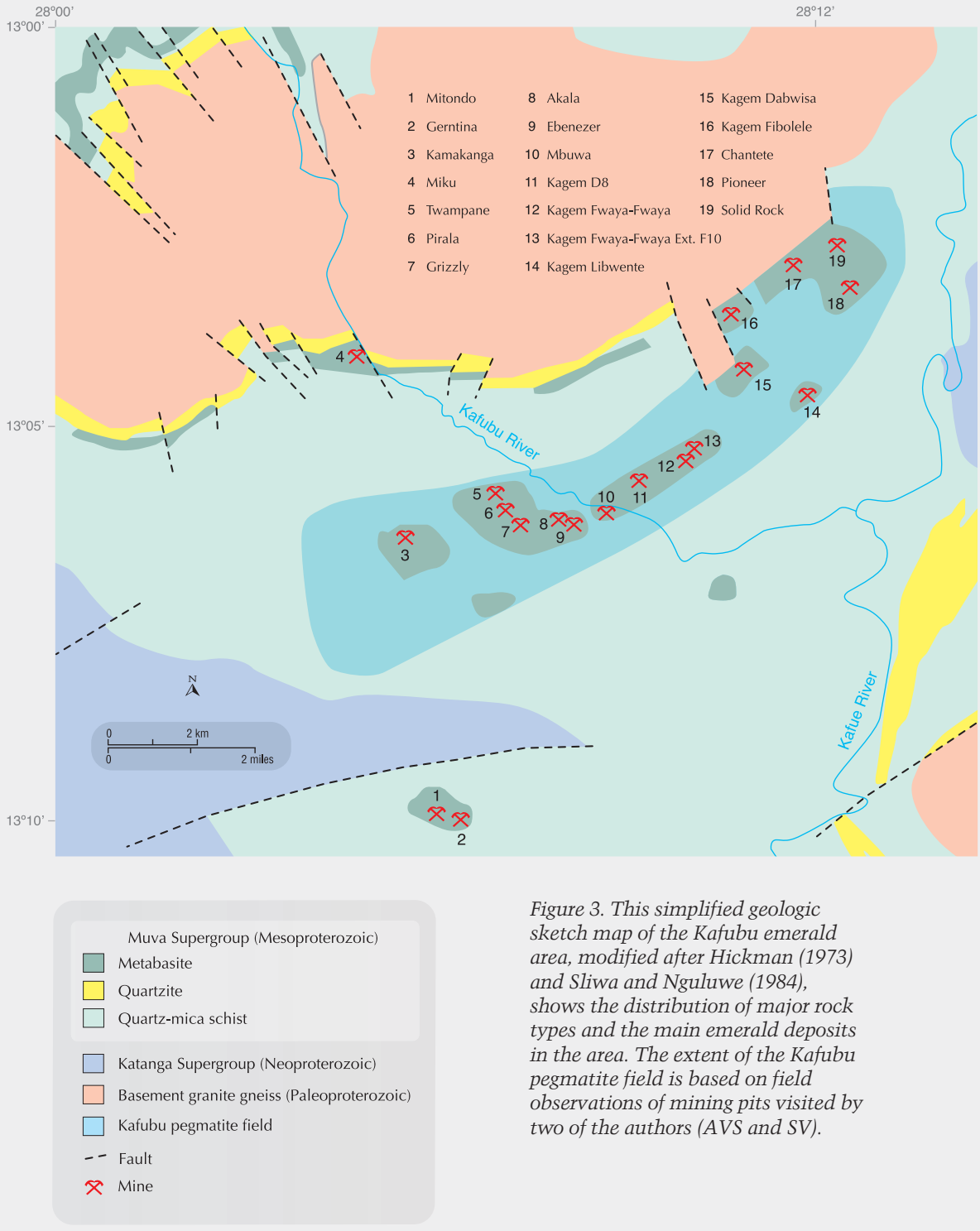

Figure 3. This simplified geologic sketch map of the Kafubu emerald area, modified after Hickman (1973) and Sliwa and Nguluwe (1984), shows the distribution of major rock types and the main emerald deposits in the area. The extent of the Kafubu pegmatite field is based on field observations of mining pits visited by two of the authors (AVS and SV).

During late stages of the Pan-African orogeny, rare-element pegmatites and some beryllium-rich granites intruded various crustal units in central, eastern, and possibly also northwestern parts of Zambia (see, e.g., Cosi et al., 1992; Parkin, 2000). In the Kafubu area, field studies at numerous mines and exploration pits indicate the existence of a major field of beryllium-bearing pegmatites and

Box A: Emerald from the Musakashi area, North-Western Province, Zambia

By Antonín V. Seifert, Stanislav Vrána, Björn Anckar, and Jaroslav Hyrsl

Figure A-1. The abandoned open-pit Hope mine in the Musakashi area reportedly was a source of emeralds. Photo by A. V. Seifert.

Figure A-2. This emerald fragment (8 × 6 mm) from the Musakashi area shows good color and transparent areas between fractures. Photo by V. Žáček.

A minor emerald "rush" occurred in 2002 at Chief Mujimanzovu's village in the Musakashi area, Solwezi district, central Zambia. In August 2002, one of the authors (BA) saw some high-quality emeralds with some Senegalese dealers in Kitwe. The color of these emeralds was significantly different from those of the Kafubu area, showing an intense bluish green reminiscent of emeralds from Muzo, Colombia. A field visit to their reported source was arranged with a Senegalese dealer, but the miners refused to grant access due to fierce disputes over the property. Visits to nearby outcrops and artisanal workings (mined for rock crystal quartz) showed the presence of abundant hydrothermal veins in the area. The European Union's Mining Sector Diversification Programme subsequently sponsored the Geological Survey Department of Zambia to map and explore the area, with field work undertaken in June 2004. By this time, it was reported that there was very little activity and the locals thought the deposit was mined out (Ng'uni and Mwamba, 2004). No in-situ emeralds were found, but small emerald fragments were recovered from eluvial lateritic soil adjacent to quartz veins at two mines (Hope and Musakashi) in the Chief Mujimanzovu village area.

When two of the authors (AVS and SV) visited the Musakashi area in July-August 2004, the pits were inactive (see, e.g., figure A-1), and data on the production and quality of the emeralds proved elusive to obtain. Nevertheless, a few emerald fragments were obtained for gemological examination and chemical analyses (see, e.g., figure A-2).

The gemological properties of three irregular polished emerald fragments (up to 6 mm in maximum dimension) were obtained by one of us (JH) using standard instruments and techniques. Refractive indices measured on two of the samples were 1.580–1.587, yielding a birefringence of 0.007. The specific gravity could not be measured accurately, due to abundant fissures in available stones. The dichroism was blue-green and yellow-green. The samples were inert to UV radiation. They had a typical chromium-type absorption spectrum and appeared red with the Chelsea filter. The most interesting characteristic was the presence in all the stones of three-phase inclusions, consisting of a bubble and a cube-shaped crystal in a liquid (figure A-3), almost identical to those commonly seen in Colombian emeralds. Note that these inclusions were very tiny—up to 0.1 mm but usually much smaller.

Mineral inclusions in these samples were examined by AVS and SV, and identified by electron microprobe. They consisted of minute crystals of sphene (titanite),

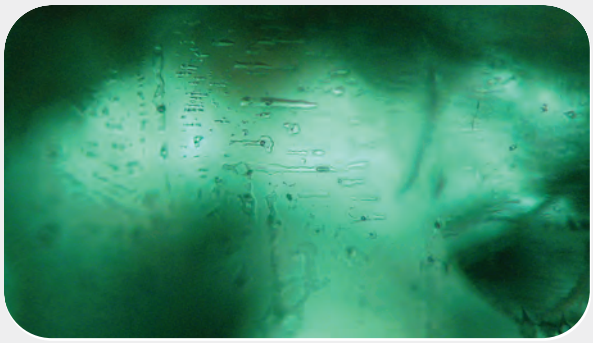

Figure A-3. All three samples of emerald from the Musakashi area contained minute three-phase inclusions that consisted of a bubble and a cube-shaped crystal that were suspended within liquid. Photomicrograph by J. Hyrsl; width of view is 0.5 mm.

Fe-oxides, Na-K feldspar, and quartz, with zeolite aggregates occurring along fissures. In comparison, the Kafubu emeralds typically contain phlogopite, actinolite, and apatite. The difference in mineral inclusions is consistent with field relations that suggest the two emerald areas are geologically unrelated.

The chemical composition of the three Musakashi samples is compared to Kafubu emeralds in table A-1. The Musakashi analyses show significantly higher Cr and V than those from Kafubu. By comparison, they also contain higher Cr and lower Mg than representative analyses of dark green emeralds from Colombia.

Although none of the authors are aware of any faceted emeralds from the Musakashi area, there appears to be potential for the production of facetable material.

TABLE A-1. Representative electron-microprobe analyses of Zambian emeralds from the Musakashi and Kafubu areas, with comparison to Colombian emeralds.

	Kafubu	Musakashi			Colombia[a]	
Oxides (wt.%)						
SiO_2	61.9–65.4	66.58	66.24	66.58	64.93	64.89
TiO_2	bdl	bdl	0.01	0.01	<0.02	0.03
Al_2O_3	12.5–17.9	15.90	15.70	15.64	15.60	18.10
Cr_2O_3	bdl–0.84	1.31	1.45	1.36	0.68	0.28
V_2O_3	bdl–0.08	0.48	0.47	0.55	1.87	0.12
FeO^{tot}	0.06–1.75	0.23	0.27	0.31	0.05	0.39
MnO	bdl–0.01	bdl	0.03	0.01	<0.02	0.05
MgO	0.27–2.90	0.73	0.72	0.72	1.27	1.24
CaO	bdl–0.12	0.02	bdl	0.01	<0.01	0.01
Na_2O	0.16–1.99	0.65	0.62	0.66	0.68	1.12
K_2O	bdl–0.27	0.03	0.02	bdl	<0.10	0.07

[a] *Representative dark green emeralds from La Pita (left column; Fritsch et al., 2002) and Somondoco (right column; Kozlowski et al.,1988). Abbreviation: bdl = below detection limit.*

hydrothermal veins that is nearly 20 km long. This field overlaps major horizons of metabasites that are enriched in chromium, resulting in emerald mineralization over a large area (again, see figure 3). Potassium-argon dating of muscovite from a pegmatite and an associated quartz-tourmaline vein gave cooling ages of 447–452 My (Seifert et al., 2004c). This corresponds to the approximate time of emerald mineralization, when the rocks cooled below 350 ± 50°C (which is the approximate temperature at which muscovite becomes "closed" to argon loss; see Viana et al., 2003).

Local Geology. Emerald miners in the Kafubu area use a local geologic vernacular that is summarized in the *G&G* Data Depository (www.gia.edu/gemsandgemology). Knowledge of this terminology is critical to understanding their observations of the geology and emerald mineralization. The emerald mineralization is directly related to the metasomatic alteration of the Cr-bearing metabasites by Be-bearing fluids derived from hydrothermal veins (see, e.g., Coats et al., 2001; Seifert et al., 2004c). For the most part, economic quantities of emerald are restricted to the phlogopite reaction zones (typically 0.5–3 m wide) between quartz-tourmaline veins and metabasite. These reaction zones locally contain aggregates of emerald (figure 4), of which a minor proportion is gem quality. Only rarely are good stones found in the quartz-tourmaline veins, or very exceptionally in less altered, partially phlogopitized host rocks (e.g., at the Grizzly mine).

Localized phlogopite reaction zones in the metabasites also were caused by emplacement of simple quartz-feldspar pegmatites, which are typically 2–10 m thick and steeply dipping. Field observations by two of the authors (AVS and SV) indicate that these pegmatites were emplaced shortly after the quartz-tourmaline veins. Since fluids from the pegmatite system contained some Be, minor emerald mineralization occurs locally in the phlogopite alteration zones associated with these pegmatites, too. The best emerald mineralization is found in phlogopite schist near intersections between the quartz-tourmaline veins and the pegmatites—particularly at the intersection between steeply dipping pegmatites and flat-lying veins.

The abundance of quartz-tourmaline veins with associated phlogopite reaction zones in the

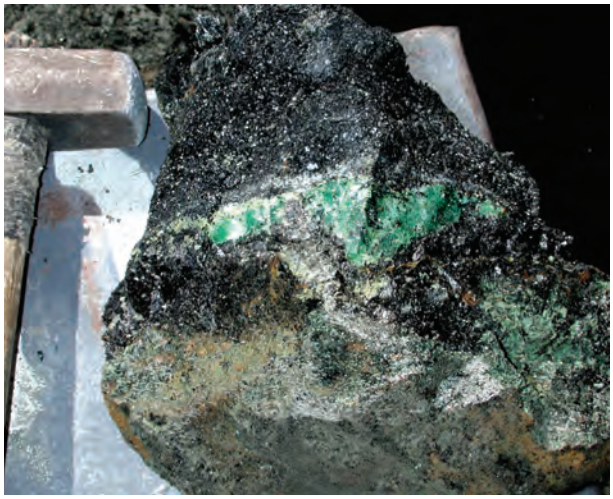

Figure 4. Emerald aggregates are locally found in phlogopite schist, as shown in this specimen from Kagem's Fibolele mine. Only a small portion of the emeralds found in these aggregates are gem quality. Photo by V. Žáček.

Kafubu area suggests a "regional" influx of hydrothermal fluids containing Si, B, K, F, and other elements (Seifert et al., 2004c). The Be-bearing fluids that altered the metabasites, causing emerald mineralization, are most likely related to a hidden granitic source. Information from a fluid inclusion study (Seifert et al., 2004c) is consistent with the results of the regional geology described above, which indicates emerald mineralization occurred at temperatures of 360–390°C and pressures of 400–450 MPa.

EXPLORATION

About 2% of the Kafubu area is currently being mined (i.e., 5 km^2), and exploration activities are limited mostly to the immediate surroundings of known deposits. The nearly omnipresent cover of residual soil (2–10 m thick) is a serious obstacle to prospecting.

Exploration methods range from witchcraft and gut feel to the use of advanced geophysical methods, core drilling, and geologic mapping. Kagem has several highly qualified geologists who methodically monitor exploration and mining activities. Smaller companies rely on local consultants who provide geologic interpretation and basic geophysical surveying (described below). Local miners, many of whom have decades of experience working the area, also are an important resource. These miners (locally called "sniffers") are experts at locating emeralds through careful field observations (e.g., quartz-rich soil uplifted in tree roots).

The target ore geology at Kafubu is favorable for magnetic surveying. This rather simple geophysical technique has been used in the area for years, and remains the main tool for emerald prospecting. A magnetic survey measures variations in the earth's magnetic field intensity over an area of interest (see, e.g., Cook, 1997). Ferromagnetic minerals and their contrasting proportions in the earth's crust produce magnetic anomalies that can help define the underlying geology of the target area. However, the expression of magnetic anomalies is highly dependent on the surrounding geology. For example, low-magnetic sedimentary rocks together with high-magnetic igneous or metamorphic rocks will typically result in distinct anomaly patterns. In the Kafubu area, the host metabasites are usually the only rocks with high contents of magnetite, which is the primary mineral causing magnetic-high readings. The metabasites are contained within generally low-magnetic quartz-muscovite schists, so the surveys usually produce easily interpreted anomaly patterns.

In addition to magnetic surveying, radiometry (see Cook, 1997) is often used at Kafubu. With this method, a gamma ray spectrometer measures U, Th, and K anomalies to distinguish different rocks on the basis of their mineralogy; it may also reveal geologic contacts and major fault structures. However, the penetration depth of this technique is very shallow, so only surface or very near-surface anomalies can be detected. Nevertheless, this technique has successfully revealed underlying pegmatites and hydrothermal veins in the Kafubu area. Combinations of magnetic highs and radiometric highs indicate a very favorable geologic setting, and such geophysical anomalies are tested by digging pits to verify the presumed occurrence of metabasites and hydrothermal veins. When favorable conditions are encountered, local geologic indicators may point toward areas with high potential for emerald mineralization.

Geochemical soil and rock sampling has been attempted in the area but has not been done systematically. The samples have been analyzed for Ni, Cr, Co, and similar elements to look for metabasites, as well as for Be, Rb, Cs, and Li as pathfinders for pegmatites and hydrothermal veins.

Although expensive and time consuming, oriented drilling exploration programs may reveal important new emerald accumulations. For example, an extensive drilling survey at a grid spacing of 25 m—carried out in the southern continuation of Kagem pit D8 in 2003—intersected a new and very promising emerald-

Figure 5. The Grizzly mine employs large earth-moving equipment in a highly mechanized operation. The excavators used in the Kafubu emerald mines typically weigh 25–30 tons and have a bucket capacity of approximately 1.6 m^3. Photo by B. M. Laurs.

bearing zone at a depth of 75 m. A similar survey in 2002 revealed additional emerald mineralization in the southeastern continuation of the Fwaya-Fwaya Ext. F10 mine (J. G. Dey, pers. comm., 2003).

So far, emerald mineralization has been mined to a maximum depth of 50–60 m (e.g., at the deepest Grizzly, Kamakanga, and Kagem mines). However, structural and lithologic criteria suggest that mineralization continues to deeper levels. Field surveys and laboratory analyses (Seifert et al., 2004c), as well as a study of the structural geology (Tembo et al., 2000), have demonstrated that the potential for substantial reserves and new emerald occurrences in the Kafubu area remains very high.

MINING

The Kafubu mining area (or Ndola Rural Restricted Area) has been subdivided into several hundred small concessions at around 100 hectares each. Most of these concessions are located in areas with unpromising geology. However, many others are in favorable areas, and a few of these have been amalgamated into larger entities such as the one operated by Kagem. The current license system has many disadvantages ("Zambia cranks up…," 2004), as these 100-hectare concessions are too small to support the investment needed to start financially viable operations, but there is no system in place to have such licenses relinquished and offered to capable mining companies. Furthermore, the area is rife with disputes and lengthy court cases that delay promising operations.

As of August 2004, the main emerald mining activities took place at the Kagem, Grizzly, and Chantete concessions. At Kagem, which at 46 km^2 is by far the largest license area, producing mines include Fwaya-Fwaya Ext. F10, Fwaya-Fwaya, Fibolele, D8, and Dabwisa. The Grizzly mine recently expanded its operations by acquiring licenses to additional concessions and investing in new machinery. The Chantete mine is also an active producer with modern equipment. Other producers include the Kamakanga, Twampane, and Akala mines, with sporadic production from the Pirala, Miku, Ebenezer, and Mitondo mines.

In June 2004, United Kingdom–based Gemfields Resources Plc started systematic exploration at its Plots 11A-1 and 11A-2 adjacent to the Pirala mine. The company is now undertaking a full feasibility study after having carried out drilling, ore body modeling, and bulk sampling. The initial results are promising, and the company expects to be in full operation by late 2005.

All the Kafubu emerald deposits are worked by open-pit mining. Because of abundant water during the rainy season (November to March), underground work is not considered an option; the groundwater level is too high for sinking shafts, as it would be too expensive to pump water continuously. Only one operator, at the Mitondo mine, has tried underground mining, but they recently ceased these activities.

Mining is done by removing the overburden rock with bulldozers, excavators, and large dump trucks (see, e.g., figure 5). At all the big pits, the miners drill

Figure 6. At the Grizzly mine, workers drill holes that will be filled with explosives to open up the area adjacent to an emerald-bearing zone. Photo by B. M. Laurs.

a series of holes (figure 6), so that explosives can be used to open the areas adjacent to the veins. Once emerald-bearing schist is exposed, mining is done manually with hammer and chisel, by so-called "chiselers." The recovered emeralds are put into cloth sacks or deposited into padlocked metal boxes. Security is a major problem during the manual extraction phase. The emerald-bearing zones must be heavily guarded at night to prevent access by the numerous illegal miners who become active after sunset. It is also not uncommon for a chiseler to cover a newly discovered emerald concentration for later nighttime excavation.

Standard washing/screening plants are used to process the ore at some of the mines. A new processing plant at the Grizzly mine was recently put into operation, with a capacity of 20 tons per hour. After crushing, the ore is washed and sized, with larger and smaller pieces separated in a rotating trommel. Additional vibrating screens further separate the material into specific size ranges for hand sorting on slow-moving conveyor belts. At Kagem, the operators rent the equipment used at the washing and sorting plant to keep costs down.

The smaller operations do not use washing plants due to a lack of funding and/or security. For instance, at the Chantete mine, 24-hour-a-day shifts keep the emerald-bearing rock moving, and all the emeralds are sorted by hand. This is done throughout the year, except during the rainy season when the pit fills with water.

Although it is expected that the Kafubu area will be able to supply a large quantity of emeralds over the next 20 years (A. Eshed, pers. comm., 2005), there is growing concern about the expenses involved in extracting them. For instance, at present the cost of running the Kagem mines is estimated to be around US$10,000 per day. The output is always uncertain; due to the irregular distribution of the emerald mineralization, it is extremely difficult to estimate reserves realistically, which makes emerald mining a high-risk business.

ENVIRONMENTAL IMPACT

A detailed study of the environmental impact of the emerald mines was performed by Seifert et al. (2004b). The mining activities affect the landscape and natural media—water, soil, rocks, and air—as well as human health. Fortunately, there are no enriched heavy metals or toxic elements in the Kafubu area.

Various environmental interactions and impacts are associated with each phase of a mine's lifespan

Figure 7. This 40 g emerald crystal fragment from the Chantete mine is illuminated from behind to show its transparency and attractive color. Photo by H. Zwaan.

Figure 8. This prismatic single crystal of emerald (slightly more than 8 cm long) was recovered from the Chantete mine. Photo by Dirk van der Marel, © Naturalis, the Netherlands.

(i.e., prospecting, exploration, mine development, mining, and closure). The most serious impacts include deforestation and vegetation removal, land degradation, increased soil erosion and siltation of watercourses, habitat loss (resulting in a reduction of biodiversity), and dangerous sites (e.g., pit walls). The amount of mined material from the entire Kafubu area that must be disposed of or stockpiled is roughly estimated at approximately 25,000 tonnes per day at current levels of activity, with a total of 70 million tonnes displaced since the 1970s.

The dozens of abandoned mines in the area do not always have negative consequences. They are filled by seasonal rainwater, and previously dry bush can benefit from the presence of a reservoir by creating new wetland ecological systems that persist throughout the year.

PRODUCTION AND DISTRIBUTION

Description of the Rough. The information in this section was derived from communications with the mine owners and from the personal experience of the authors. Much of the emerald rough is recovered as fragments that show only a few crystal faces (e.g., figure 7), but well-formed hexagonal crystals are sometimes produced (figure 8). Typically, though, these are broken segments that rarely have natural flat (pinacoidal) terminations. Also seen are emerald clusters or aggregates (figure 9), which may show well-formed crystals with perfectly developed terminations, as well as hexagonal prisms with irregular terminations. The aggregates may contain several to dozens of individuals within the host schist. Step-growth crystal surfaces are frequently present, caused by abrupt changes in diameter. The surface quality of the crystal faces is often rough, but it may be glassy smooth.

The color of the emerald crystals ranges from light bluish green to dark green. Very pale green or blue (rarely colorless) beryl also is found. As with emeralds from other localities, color zoning is common. Larger crystals typically have a core that is light yellowish green to greenish blue surrounded

Figure 9. This cluster of well-formed emerald crystals was found at the contact of a quartz vein with phlogopite schist at the Chantete mine. The width of this specimen is 9 cm. Photo by Dirk van der Marel, © Naturalis, the Netherlands.

by a deep green rim; other crystals may show both a core and rim that are deep green, with internal zones of light and/or medium green.

The crystals typically range from less than 1 mm to several centimeters long, with pieces exceeding 10 cm encountered occasionally. The largest crystal observed by the authors was about 14 cm long and weighed over 3 kg (see, e.g., figure 25 inset in Laurs, 2004). According to a local mine manager, exceptionally large emerald crystals up to 60 cm long were found in the phlogopite schist at the Kamakanga Old Pit during the 1980s.

Production of the Rough. Emerald mineralization is very irregular, with the crystals often aggregated together (figure 4). These local concentrations may have grades of several kilograms of emerald per ton of ore rock. More typical is a dispersed mineralization of a few grams per ton of ore.

Run-of-mine (ROM) emerald typically yields only a small percentage of material that can be faceted. Most of it is of bead to cabochon quality. According to information supplied by T. Schultz (pers. comm., 2005) and Milisenda et al. (1999), a typical 10 kg of ROM emerald from a favorable deposit would yield about 5 g of extra-fine material, about 100 g of fine material, about 300 g of good material (in terms of both color and clarity), about 600–800 g of material with good color but included, about 3,000 g of low-quality material, and the remaining 6–7 kg of very low commercial value.

At Kagem, an average production of 300 kg (including low-grade emerald and beryl) every 2–3 months contains 10% facetable and cab-quality emeralds, with the remainder usable for beads and carvings. Typically, the emeralds occur as crystals up to 60 g each, but occasionally crystals as large as 1 to 3 kg are found. However, these large specimens usually contain only 1–2% cuttable material (A. Eshed, pers. comm., 2005). In terms of quality, F10 is currently the best-producing Kagem mine, with better (higher clarity) crystals than the former top producer, Fwaya-Fwaya (I. Eliezri, pers. comm., 2005). The Fibolele and D8 mines generally produce "medium-quality" stones—that is, good colors, but included, both facetable and cab quality. The Dabwisa mine mainly produces cabochon material, some of which is referred to as "metallic green" (caused by "rusty" looking inclusions; A. Eshed, pers. comm., 2005).

The Grizzly mine produces a quantity similar to that from the Kagem mines but generally bigger pieces (often 50 g to 1 kg), although most are of "medium quality." Large crystals also are found. Production at the Chantete mine is typically 150–300 kg per month, and large crystals are produced occasionally there as well. Only about 10% is suitable for cutting, and just 1% is facet grade (see, e.g., figure 7). Stones from this mine tend to be somewhat lighter in color than those from elsewhere in the Kafubu area.

Production of rough reportedly exceeded US$100 million in the late 1980s (Milisenda et al., 1999). More recently, the value of emerald production from the Kafubu area was reported to be about US$20 million annually—according to 2002 statistics from the Export Board of Zambia for the officially declared export value of rough emerald. A conservative estimate is that at least another US$5 million worth of rough is smuggled out of Zambia (Douglas Ng'andu, DN Consulting Associates Ltd., Kitwe, pers. comm., 2005), although some sources (mainly the Zambian media) place the number much higher. However, it is difficult to imagine where such large quantities of emerald would originate, given that there are only two large operators and the presence of secret "bonanza" mines is not realistic.

Distribution of the Rough. Most of Zambia's emeralds are exported to India, mainly for use in that country's domestic market, and to Israel for international distribution. According to D. Tank (pers. comm., 2005), India receives 80% of Zambia's emerald production by weight, and 70–75% by value, with the cutting done in Jaipur. Israeli buyers usually purchase the higher-quality material.

The larger mining operators have well-established trading arrangements. For example, Kagem offers their production four times a year at a closed-tender auction in Lusaka. The dates are flexible, depending on when sufficient material is available. The very small operators and illegal miners rely on local traders, who are mainly of West African origin (e.g., Senegal and Mali) and often supply them with food and other necessities in exchange for emeralds.

The Informal Local Market. Rough emeralds are frequently traded on the streets of Lusaka and Kitwe, usually as run-of-mine material sold by illegal miners. Occasionally, large top-quality emeralds also turn up on the informal street market.

Buyers who visit Zambia should be aware of various scams. Green glass (stolen from local traffic lights) is molded to simulate hexagonal emerald

crystals, and quartz crystals are colored by green marker pens. While these imitations are easy to identify, there also are more clever imitations such as pieces of Russian hydrothermal synthetic emerald that are carefully coated in clay and mica.

Production and Sorting of Cut Emeralds. Gemstar Ltd., based in Ramat Gan, is the largest manufacturer of Zambian emeralds for the international market; it consumes most of the higher-quality rough material. Gemstar produces 2,000–3,000 carats per month of cut emeralds, from approximately 15,000 carats of rough. As an example of how the company approaches the rough from a commercial viewpoint, the following case was demonstrated to the senior author: While evaluating a 312 ct piece of rough that was of very good quality, the manufacturer decided that, instead of cutting this piece into a few stones weighing 5–10 ct, he would aim for smaller stones of high clarity, because there is strong demand for such emeralds. In the preform phase, 105 carats were recovered from the piece of rough, from which 60 carats of faceted gems (0.50–5 ct) were produced—for a yield of only 20% of the original high-quality crystal. An example was also provided for medium-quality (i.e., more included) rough: Four pieces weighing a total 84 carats had a yield of 20% after preforming and only 10% after faceting (including very small stones with little commercial value). For cabochon-grade material, the recovery is sometimes not more than 7%.

As explained by Daniel Madmon, manager of Gemstar's cutting factory, the typical cutting procedure is outlined below:

Figure 10. At Gemstar, after a piece of rough has been assessed, it is typically sawn into several transparent pieces for faceting. Photo by H. Zwaan.

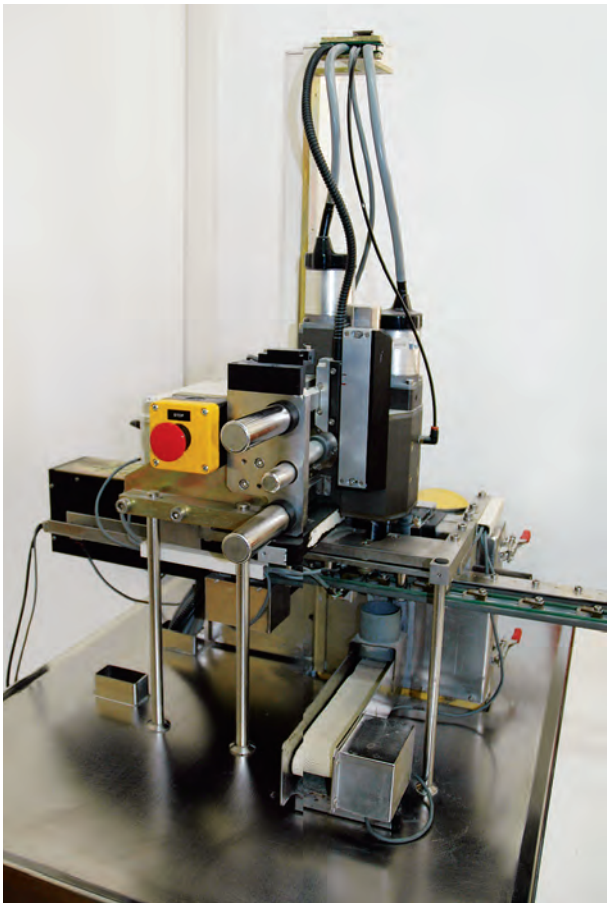

Figure 11. The sawn pieces of emerald are evaluated by the Robogem machine to predict the maximum yield and preshape the rough. Photo courtesy of E. Eliezri.

1. Using a strong lamp, the cutter assesses how and where to trim the rough, and the sawing is done carefully by hand (figure 10).
2. The sawn pieces go to the office for evaluation, and the cutting style is chosen according to demand.
3. Next, the sawn pieces are sent to a computerized robot, called "Robogem" (figure 11). Manufactured by Sarin Technologies Ltd., this equipment uses the Sarin DiaExpert system (as described by Caspi, 1997) to measure each sawn piece and predict the best possible yield. The robot is then used to make the girdle of each stone.
4. Once returned to the factory, the emerald preforms are placed on a dop and faceted by hand (figure 12), rather than by machine, because a "soft touch" is needed for emeralds. First, the

Figure 12. After they have been preshaped by Robogem, the emeralds are cut and polished by hand, using precise cutting and polishing wheels and equipment. Photo by H. Zwaan.

table and crown facets are cut and (with the girdle) polished.

5. The cutter then turns the stone on the dop and cuts/polishes the pavilion side. Taking an emerald cut as an example, the cutter places a maximum of three steps on the pavilion to get the best color, with more steps (up to four or five) used if greater sparkle is the goal.

Figure 13. At Gemstar, emeralds cut in calibrated sizes are sorted by color and clarity into numerous categories. Photo by H. Zwaan.

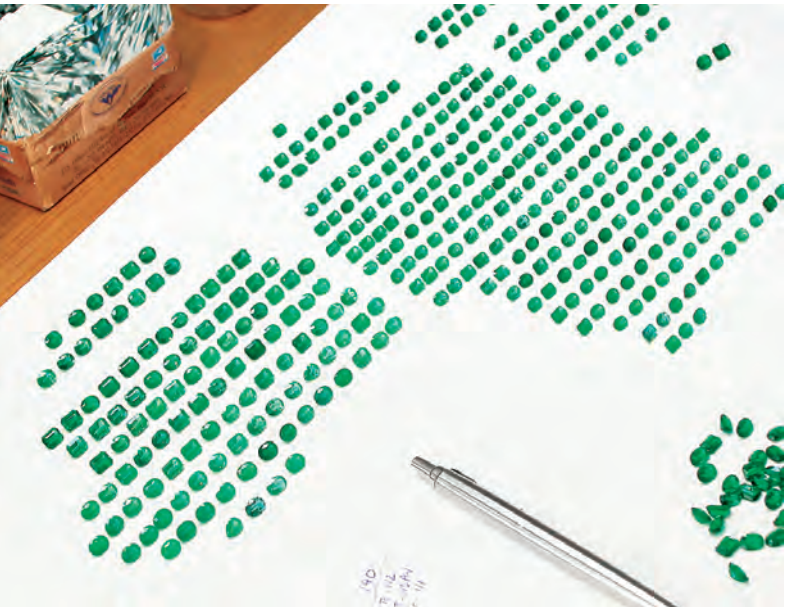

6. Once cutting and polishing is complete, the dop is gently iced so that the emerald can be easily removed. Subsequently, the finished gem is cleaned in an alcohol solution.

Each step of the cutting process is monitored by the master cutter, so that minor adjustments can be made when necessary. After polishing, stones with fissures are clarity enhanced by Gemstar using paraffin oil (i.e., mineral oil), a near-colorless transparent oil that the company has used for nearly 30 years. Gemstar declares at the time of sale that its emeralds are enhanced in this way. Resins like Opticon are never used.

Commercial production is done in calibrated sizes, such as 5 × 3, 6 × 4, 7 × 5, 8 × 6, and 10 × 8 mm. Typically, these are divided equally between emerald and oval cuts, although other shapes, such as hearts and pears, also are produced.

Next, the stones are sorted according to color and clarity into numerous categories (figure 13), based on master sets. Gemstar keeps an inventory of about 35,000 carats, so they can repeatedly produce the same colors, makes, and sizes. The steady availability of calibrated sizes of consistent quality is extremely important to customers, and the Zambian emerald is prized for such consistency (A. Eshed, pers. comm., 2005).

Commercial goods typically weigh up to 5 ct. Zambian emeralds over 10 ct are rare (again, see figure 1). During a visit to Ramat Gan, the senior author encountered a rare 14.29 ct medium-dark green stone (figure 14) that was only slightly included.

Consuming Countries. As mentioned before, most Zambian emeralds end up in India, where they are cut and distributed, mainly to the domestic market. In Israel, Gemstar Ltd. sells 70% of its stones to the U.S., 15% to the Far East, and roughly 15% to Europe. It is expected that in the future the growing markets will be in China, Russia, and eastern Europe.

MATERIALS AND METHODS

For this study, we examined a total of 127 emeralds (0.07–5.69 ct), of which 69 were faceted and 2 were cabochon cut. Almost all the 56 rough samples were transparent and suitable for faceting. At least two windows were polished on each rough sample; the resulting pieces ranged from 0.46 to 6.98 ct. The samples were obtained from several mines: 34 from

Figure 14. This exceptional Zambian emerald weighs 14.29 ct. It shows a deep "Zambian" bluish green color and is only slightly included. Courtesy of Gemstar Ltd.; photo by H. Zwaan.

Figure 15. The emeralds studied for this report represented a range of color, as evident in these samples from the Kagem mines (0.55–5.69 ct). Photo by Jeroen Goud, © Naturalis, the Netherlands.

the Chantete mine, 51 from the Kagem mines (specific pits not known), and one from the Kamakanga mine. In addition, a thin section was cut from a light bluish green emerald from the Mbuwa mine; this emerald, which was not of gem quality, was hosted by a quartz-tourmaline vein in phlogopitized metabasite. The other 40 samples were from unspecified mines in the Kafubu area.

All of the rough samples and 59 of the cut stones (see, e.g., figure 15) were examined at the Netherlands Gemmological Laboratory (NGL). Twelve faceted emeralds (0.22–4.28 ct) were examined at GIA in Carlsbad; these were cut from rough produced at the Chantete mine during the 2004 mining season (see, e.g., figure 16).

Standard gemological properties were obtained on all the emeralds. We used a GIA GEM Instruments Duplex II refractometer (at GIA) and a Rayner refractometer with an yttrium aluminum garnet prism (at NGL), both with near-sodium equivalent light sources, to measure the refractive indices and birefringence. Specific gravity was determined by the hydrostatic method. We tested the samples for fluorescence in a darkened room with four-watt long- and short-wave UV lamps. Absorption spectra of the stones examined at NGL were observed using a System Eickhorst Modul 5 spectroscope with a built-in light source. Internal features were observed with a standard gemological microscope; in some cases, a polarizing (Leica DMRP Research) microscope was used as well. In 29 samples, we analyzed inclusions with Raman spectroscopy using 514 nm laser excitation and two instruments: a Renishaw 2000 Ramascope (3 samples at GIA) and a Renishaw Invia (26 samples at the CCIP French Gemmological Laboratory in Paris). Polarized absorption spectra of 15 representative samples examined at NGL were taken with a Unicam UV540 spectrometer, in the range of 280–850 nm. Spectroscopy of the 12 samples studied at GIA was performed with a Hitachi U-4001 spectrophotometer (oriented UV-Vis spectra, range 280–850 nm) and a Nicolet Magna-IR 760 spectrometer (mid-IR spectra, 400–6000 cm^{-1}). Additional mid-IR spectra were taken of 12 representative samples at NGL using a Thermo Nicolet Nexus FT-IR-NIR spectrometer.

EDXRF spectroscopy was performed on the 12

Figure 16. Many Zambian emeralds are an attractive saturated medium bluish green, as evident in this selection from the Chantete mine (0.66–1.35 ct). Courtesy of Chantete Emerald Ltd.; photo © GIA and Jeff Scovil.

GIA samples with a Kevex Omicron instrument. The instrument was operated at a voltage of 15 kV without a filter for low-Z elements, with an aluminum filter at 20 kV for transition metals, and with an iron filter at 25 kV for heavier elements. An Eagle μProbe EDXRF spectrometer was used at NGL to analyze the composition of surface-reaching inclusions on the pavilions of 16 faceted samples. This instrument has a focus spot of 200 × 200 μm and a beam diameter of 300 μm. A voltage of 25 kV and a count time of 100 seconds were used for each measurement.

Quantitative chemical analyses were carried out on 27 selected emeralds from the Kagem and Chantete mines at two electron microprobe facilities—the Institute of Earth Sciences, Free University of Amsterdam, the Netherlands (JEOL model JXA-8800M) and the University of New Orleans, Louisiana (ARL SEMQ instrument). In Amsterdam, 78 spot analyses were performed on the table surfaces of 12 light to dark bluish green faceted emeralds from the Kagem mines and 3 polished fragments from the Chantete mine. Twenty analyses were done on surface-reaching inclusions. Analyses were performed at 15 kV, with a beam current of 25 nA and a spot size of 3 μm. The count time for the major elements was 25 seconds, and for the trace elements, 36 seconds (except 50 seconds were counted for V, Cr, F, and Rb). From two to 16 spots per sample were analyzed. In New Orleans, the tables of 12 faceted Chantete emeralds were analyzed at 15 kV, with a beam current of 15 nA and a spot size of 2 μm, and a count time of 45 seconds for each element. Three spots per

TABLE 1. Physical properties of emeralds from the Kafubu area, Zambia.[a]

Color	Colors range from light to dark green to slightly bluish to bluish green; typically a saturated bluish green with a medium to medium-dark tone
Clarity	Very slightly to heavily included
Refractive indices	n_o = 1.585–1.599; n_e = 1.578–1.591 n_o = 1.589–1.597; n_e = 1.581–1.589[b] n_o = 1.602; n_e = 1.592[c]
Birefringence	0.006–0.009 (0.008[b], 0.010[c])
Optic character	Uniaxial negative
Specific gravity	2.71–2.78 (except one 0.22 ct sample, which gave a value of 2.81) 2.69–2.77[b]
Pleochroism	Strong yellowish green (o-ray) and bluish green (e-ray); some stones showed strong greenish yellow (o-ray) and greenish blue (e-ray)
Fluorescence	Usually inert to long- and short-wave UV radiation; sometimes faint green to long-wave
Chelsea filter reaction	No reaction or light pink to red (deep green samples)
Absorption spectrum	Some absorption between 580 and 630 nm; distinct lines at approximately 636, 662, and 683 nm
Internal features	• "Feathers" in flat, curved, (rarely) conchoidal forms or undulatory/scalloped shapes • Partially healed fissures with various shapes of two- and three-phase fluid inclusions, but typically equant or rectangular • Isolated negative crystals containing CO_2 and CH_4 • Parallel oriented decrepitated inclusions appearing as silvery disks or brownish spots, depending on the lighting • Mineral inclusions (this study): randomly oriented actinolite needles, platelets of phlogopite or rare chlorite, equant to columnar dravite, fluorapatite, magnetite, hematite, chlorite, quartz, fluorite; carbonates (magnesite/siderite, ferroan dolomite, ankerite and calcite); niobian rutile, pyrite, talc, zircon, barite, albite, calcite, sphene (titanite), and beryl • Characteristic inclusions described by other authors: phlogopite/biotite, actinolite-tremolite, and square- and rectangular-shaped fluid inclusions (Milisenda et al., 1999); phlogopite, glauconite, talc, apatite, quartz, and Fe-Mn and Fe-Cr oxides (Moroz and Eliezri, 1999); apatite, quartz, chrysoberyl, margarite, muscovite, and rutile or brookite (Graziani et al., 1983); tourmaline, limonite, magnetite, mica, rutile, hematite, and apatite (Koivula, 1982; 1984), and also chrysotile (Gübelin and Koivula, 1986) • Cavities, representing dissolved columnar mineral inclusions • Either homogeneous color distribution or medium to strong color zoning may occur (as planar zones oriented parallel to the prism faces)

[a] *All data are from the present study unless otherwise noted.*
[b] *Data from Milisenda et al. (1999), obtained from an unspecified number of samples that they described as representative. Other data on refractive indices, birefringence, and specific gravity, such as reported by Graziani et al. (1983) on a single sample, and the average values given by Campbell (1973) for Zambian emeralds, fall within the ranges that are indicated.*
[c] *Data from Schmetzer and Bank (1981) on one dark bluish green sample.*

sample were analyzed.

In addition, three emerald fragments from the Musakashi area (box A) were analyzed using a Cameca SX 100 electron microprobe (15 kV, 40 nA) at Masaryk University, Brno, Czech Republic.

GEMOLOGICAL PROPERTIES

The gemological properties are summarized in table 1, with details described below.

Visual Appearance. The emeralds showed a wide variety of colors, ranging from green to slightly bluish green to bluish green with a light to dark tone (figure 15). Many were an attractive saturated bluish green with a medium to medium-dark tone (figure 16). Typically, the color was evenly distributed, although we saw strong color zoning in some crystals and polished material. Color zoning in the faceted stones was best seen from the side, when looking parallel to the table through the pavilion.

Physical Properties. Roughly 70% of the stones tested showed refractive indices of n_o = 1.591–1.595 and n_e = 1.583–1.587. Some light green stones showed values lower than 1.583, and some dark green stones had R.I.'s above 1.595. The birefringence of most of the emeralds ranged between 0.007 and 0.008. Only one stone had a birefringence of 0.006, and only two stones showed 0.009.

Specific gravity values ranged from 2.71 to 2.78. The majority of the stones (78%) had an S.G. between 2.72 and 2.76.

The emeralds were typically inert to long- and short-wave UV radiation, except for a few samples that fluoresced faint green to long-wave UV. All of the emeralds with more saturated colors appeared pink to red under the Chelsea filter; the other samples showed no reaction. Dichroism was strong, in yellowish green and bluish green; or even stronger, in greenish yellow and greenish blue. Most of the emeralds, even the light-colored stones, showed well-defined absorption spectra when viewed with the handheld spectroscope. The spectra showed some absorption between 580 and 630 nm, and distinct lines at approximately 636, 662, and 683 nm. The violet range (beyond 430 nm) was completely absorbed. A few light-colored emeralds showed a weaker spectrum with only a clear line at 683 nm.

Microscopic Characteristics. The stones were very slightly to heavily included. The most obvious clarity characteristics were fractures, partially healed fissures, fluid inclusions, needles, and occasional brown flakes.

Fractures and Fluid Inclusions. The most conspicuous inclusions consisted of "feathers" and partially healed fractures, which both exhibited wide variations in appearance. Feathers had flat, curved, or rarely conchoidal forms with mirror-like reflections, or undulatory/scalloped shapes with a white appearance caused by rough surfaces. Less commonly, the feathers were present in parallel formations or in tight clusters with no preferred orientation. One sample from Chantete contained larger fractures that locally showed blue "flash-effect" colors due to filling with a foreign organic substance.

Partially healed fractures were marked by planar groups of equant, elongated, wispy, or irregularly shaped fluid inclusions that often showed low relief and contained relatively small bubbles (figure 17), indicating that they are probably H_2O rich (e.g., Samson et al., 2003). Partially healed fractures also were represented by arrays of pinpoints that formed parallel lines (see, e.g., figure 18) or "fingerprints."

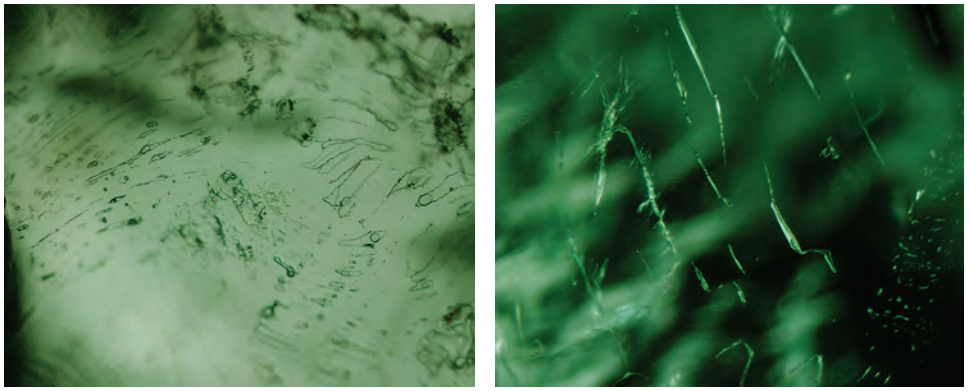

Figure 17. Irregularly shaped (left) and wispy (right) fluid inclusions, such as those present in these two emeralds from the Chantete mine, were widespread in the Zambian emerald samples. Photomicrographs by H. Zwaan; magnified 50× and 55×, respectively.

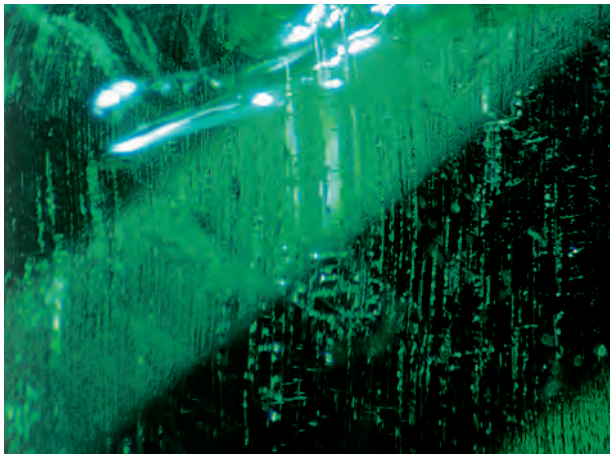

Figure 18. Parallel arrays of secondary fluid inclusions were relatively common in the Chantete emeralds, as were fractures of various sizes. Photomicrograph by J. I. Koivula; magnified 10×.

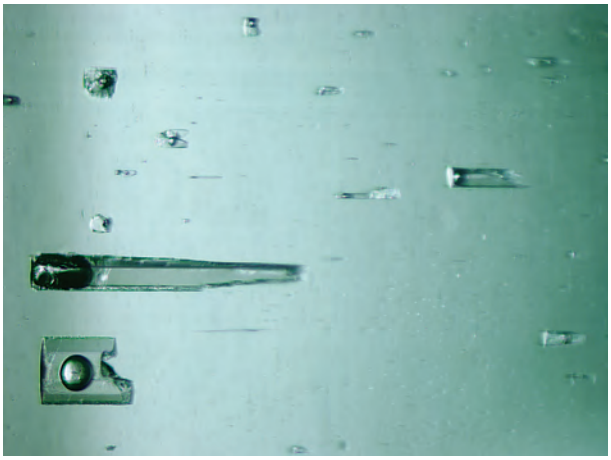

Figure 19. Rectangular pseudosecondary two-phase inclusions, typically present in healed fissures in many Zambian emeralds, mainly contain H_2O (liquid) and CO_2 (gas). Photomicrograph by H. Zwaan; magnified 100×.

Many of the Zambian emeralds had healed fissures consisting of pseudosecondary rectangular to square fluid inclusions (a hundred or more microns) that each contained a bubble (figure 19). These inclusions generally contained either two phases (liquid and gas, mainly H_2O [by inference] and CO_2 [identified by Raman analysis]) or three phases (liquid, gas, solid), which often looked like two-phase inclusions because the solids were only clearly visible with crossed polarizing filters (figure 20). The solids were tentatively identified by optical means as carbonates. In heavily included emeralds, the healed fissures were often accompanied by minute fluid inclusions, causing a milky translucency. Fluid-filled tubes oriented parallel to the c-axis were commonly seen in light-colored emeralds (figure 21), but they were rare in the saturated medium to dark green stones.

Compared to the abundant pseudosecondary fluid inclusions in healed fissures, primary inclusions were less common, and were not present in every stone. They formed isolated negative crystals with a roughly hexagonal outline and high relief in transmitted light (figure 22). They appeared to be CO_2-rich, each with a large bubble occupying most of the available space. Raman analysis confirmed that these inclusions contained CO_2 as well as CH_4 (an example spectrum is in the *G&G* Data Depository). Other isolated, irregular-shaped primary three-phase fluid inclusions, containing an obvious solid phase, were very rare (figure 23).

Parallel planes of decrepitated inclusions, containing remnants of fluid, were observed in a number of stones. When viewed with oblique illumination, these features only showed up clearly in a specific orientation when the light was properly reflected; in transmitted light, they appeared as parallel faint brownish spots with a vague hexagonal outline (figure 24).

Mineral Inclusions. Mineral inclusions were common in the lower-clarity Zambian emeralds. Colorless needles with diamond-shaped cross sections were visible in many of the stones (figure 25) and were identified as actinolite in five of the sam-

Figure 20. Many rectangular three-phase inclusions look like two-phase inclusions (left), because the solid phase (carbonate) only became apparent when viewed with crossed polarizers (right). Photomicrographs by H. Zwaan; magnified 100×.

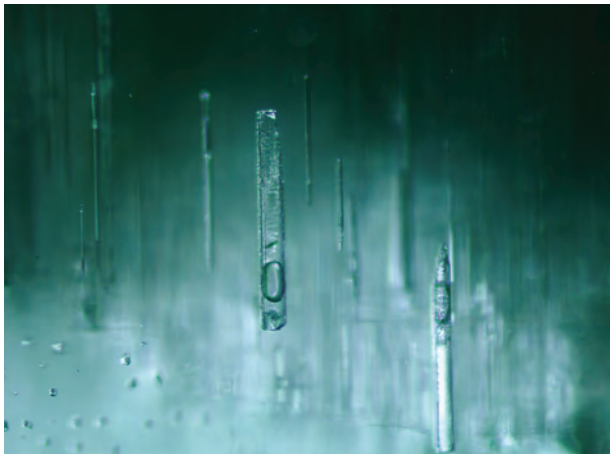

Figure 21. Parallel-oriented tubes commonly were present in the light-colored emeralds. In this particular sample, the tubes are seen only in the light green portion. Photomicrograph by H. Zwaan; magnified 100×.

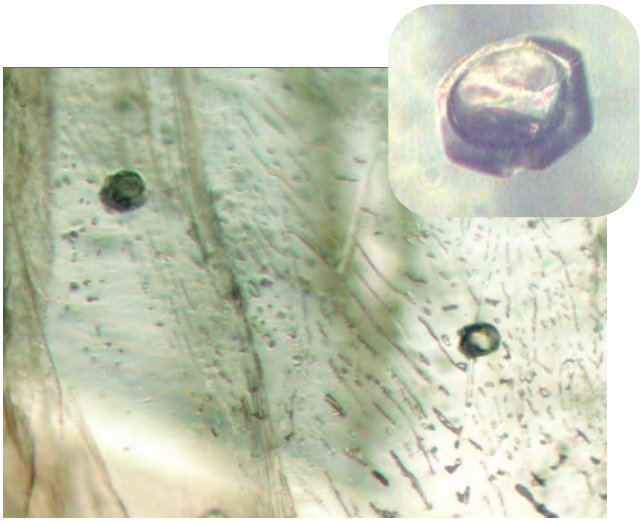

Figure 22. Primary inclusions appear as small isolated negative crystals in the Zambian emeralds, with high relief evident in transmitted light at 50× magnification. The "curtain" behind the two negative crystals is a partially healed fissure. Only under strong magnification could a large bubble be observed inside each cavity (see inset, magnified 250×). Photomicrographs by H. Zwaan.

ples by Raman analysis. Two microprobe analyses of a surface-reaching inclusion gave Mg/(Mg + Fe^{2+}) ratios of 0.77 and 0.78, indicating a Mg-rich actinolite (per the classification of Leake et al., 1997). This was similar to the composition of actinolite in the host metabasites (ratio of 0.78–0.86; Seifert et al., 2004c). Some of the actinolite needles were surrounded by material with a fuzzy appearance (probably microfractures; figure 26). The needles were typically straight, although a needle in one emerald from the Chantete mine was obviously curved.

Also common were pale to moderate brown platelets (figure 27) that provided Raman spectra consistent with biotite/phlogopite. Microprobe analyses of eight grains in four different emerald samples gave phlogopite compositions, which is in agreement with the compositions of micas in the altered metabasite host rock as documented by Seifert et al. (2004c) and with the composition of an inclusion in a "bluish green Zambian emerald" given by Moroz and Eliezri (1999). In a few stones that contained a fair amount of phlogopite, dark green mica also was found. One such inclusion (figure 28) was identified as chlorite by Raman analysis.

Less abundant than actinolite or phlogopite were high-relief, dark brown to black, equant to columnar crystals (figures 25 and 29). These inclusions had a rounded triangular cross section that is typical of tourmaline. Raman spectra of two such inclusions were consistent with schorl-dravite tourmaline. A semiquantitative EDXRF analysis of the crystal in figure 29 revealed nearly twice as much MgO as FeO, and little Ca, identifying it as dravite. This is consistent with earlier studies of tourmaline from the Kafubu area by Koivula (1984) and Seifert et al. (2004c), who found Fe-rich or Ca-Fe rich dravites, with individual crystals showing significant compositional variations.

Apatite was identified by Raman analysis in four emeralds from the Kagem mining area. It usually formed colorless euhedral crystals (figure 30) or small colorless grains with irregular surfaces. One

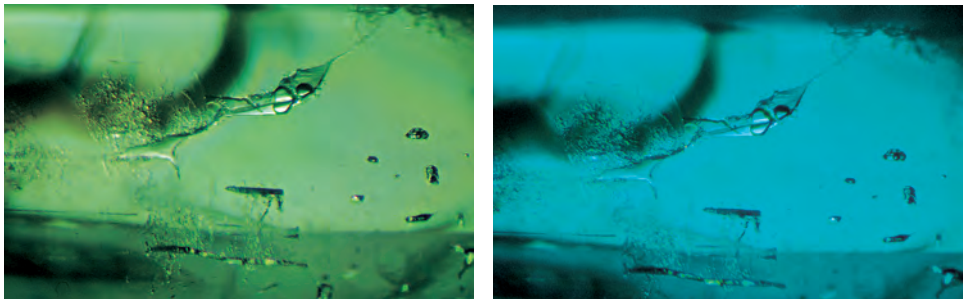

Figure 23. This primary three-phase fluid inclusion was observed in a Chantete emerald. Rotating the microscope's polarizer showed the yellowish green (left) and greenish blue (right) dichroic colors of the emerald. Photomicrographs by J. I. Koivula; magnified 15×.

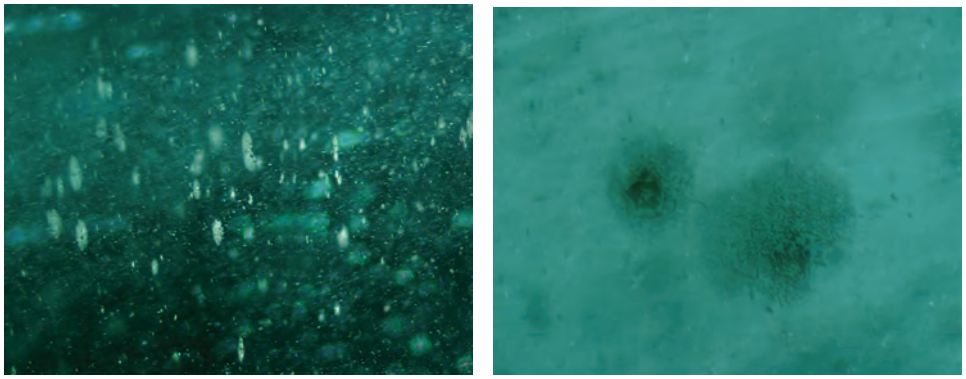

Figure 24. With oblique illumination, thin parallel planes of decrepitated inclusions, with fluid remnants, were commonly seen in the Zambian emeralds (left). When viewed in transmitted light, however, they appeared as faint brownish features with a vague hexagonal outline (right). Photomicrographs by H. Zwaan; magnified 50× (left) and 200× (right).

heavily included dark bluish green emerald contained numerous hexagonal prisms of apatite, with two crystals at the surface identified by microprobe analysis as fluorapatite. Interestingly, this tiny inclusion itself contained even smaller inclusions of actinolite and magnetite (figure 31). Minute opaque black "crumbs" and larger euhedral-to-anhedral opaque grains, which formed skeletal features in parallel planes (figure 32) and had a submetallic luster, were identified as magnetite by both Raman and microprobe analyses. In a few emeralds, brown-red inclusions with similar skeletal shapes were identified by Raman analysis as hematite (again, see figure 32). This suggests the presence of martite, a variety of hematite that is a pseudomorph after magnetite.

Cavities that appeared to represent casts of dissolved mineral inclusions with a euhedral columnar habit were seen in a few samples (figure 33).

Small, slightly rounded, euhedral transparent crystals were encountered in some emeralds. In most cases, they were too deep within the stone to be identified by Raman analysis. One sample showed many of these crystals, both isolated and in clusters. Some crystals had very low relief and were doubly refractive, whereas others had higher relief and were isotropic. At the surface, a few crystals of both types were identified by microprobe as quartz and fluorite, respectively (figure 34). In one sample, between a quartz and a fluorite crystal, three carbonates also were identified: a magnesite/siderite mixture, ferroan dolomite, and ankerite. Interestingly, these carbonates contained a fair amount of Cr (e.g., up to 1.34 wt.% Cr_2O_3 in the ankerite). A small beryl inclusion seen in association with these carbonates contained less Mg and Fe than the emerald host. Raman analysis confirmed the presence of additional carbonate inclusions in a few other stones.

Other rare inclusions identified in the Zambian

Figure 25. Colorless needles of actinolite in a Chantete emerald appear brownish yellow in this image taken between crossed polarizers. The dark grain between the two actinolite needles in the center of the image is probably tourmaline. A network of fractures also is present in this view. Photomicrograph by J. I. Koivula; magnified 13×.

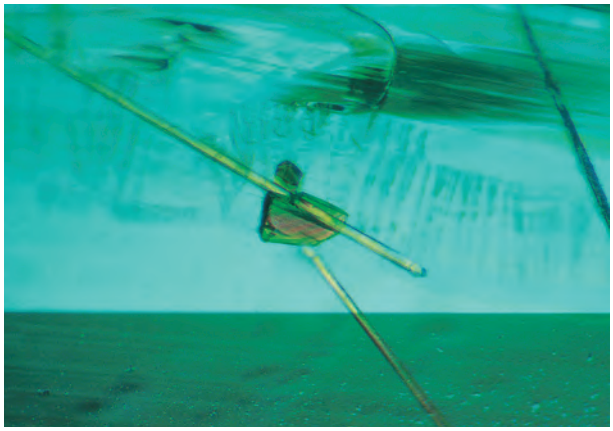

Figure 26. A fuzzy-looking white "coating" of micro cracks and/or fluid inclusions hides the identity of the rod-shaped solid inclusion inside this Chantete emerald. Similar coatings were seen associated with the needles that were identified as actinolite in other samples. Photomicrograph by J. I. Koivula; magnified 15×.

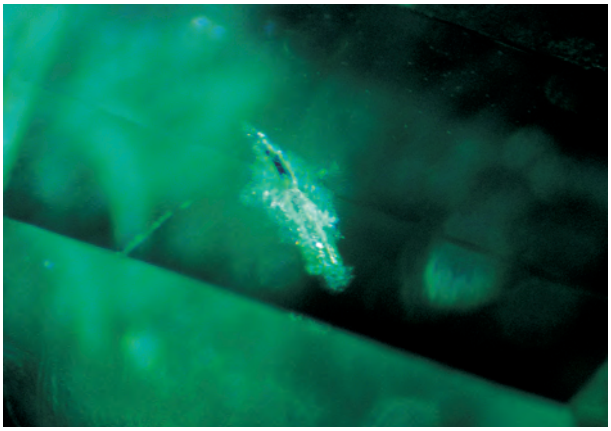

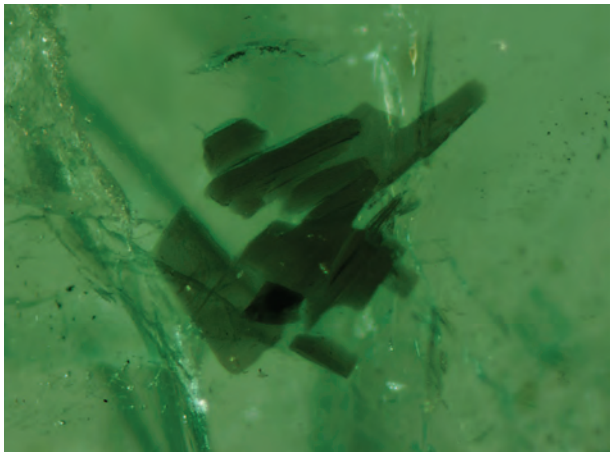

Figure 27. Platelets of phlogopite, as seen here in one of the Chantete emeralds, are quite common inclusions in Zambian emeralds. Photomicrograph by H. Zwaan; magnified 80×.

Figure 28. A few stones contained chlorite—like the crystal in the center here—as well as phlogopite. Photomicrograph by H. Zwaan; magnified 80×.

emeralds were pyrite and talc, present as fairly large crystals in one heavily included sample; very small grains of zircon, which were also observed in some phlogopite inclusions, where they had caused dark brown radiation halos; and minute grains of barite, albite, and calcite. In one cut emerald from the Kagem mining area, calcite was present in surface-reaching fractures. A small euhedral crystal of sphene (titanite) was found in one faceted emerald; its identity was confirmed by Raman analysis. All of the other inclusions in this paragraph were identified by a combination of visual appearance and EDXRF spectroscopy, microprobe, or Raman analysis.

In the thin section of the Mbuwa mine emerald, some reddish orange inclusions were identified as niobian rutile (figure 35). Rutile inclusions in Zambian emerald have previously been described by various authors (e.g., Graziani et al., 1984; Gübelin and Koivula, 1986; Seifert et al., 2004c), but the reddish orange color in the thin section suggested the presence of Fe^{3+}, Nb, and/or Ta. Raman analysis showed a rutile spectrum with fundamental

Figure 29. Equant black-appearing crystals of dravite (Mg-bearing tourmaline) also were observed, as seen here in an emerald from the Kagem mining area; the crystal with the rounded triangular cross section shows the typical crystal habit of tourmaline. Most of the tourmaline crystals observed appeared to have grown where actinolite needles intersect. Photomicrograph by H. Zwaan; magnified 80×.

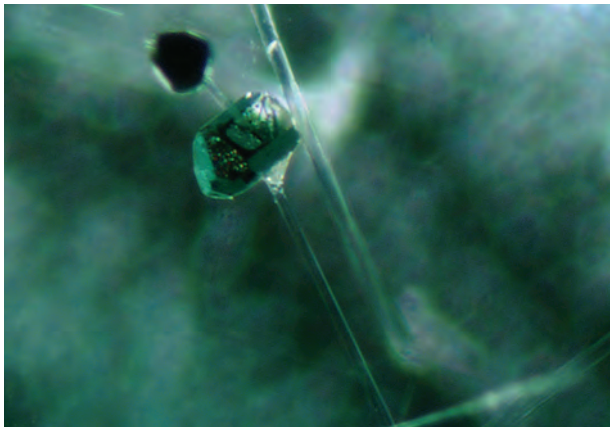

Figure 30. Large and small euhedral apatite crystals are seen in this emerald from the Kagem mining area. The apatite inclusions are transparent and show virtually no color. The size (1.0 mm long) of the large crystal is quite unusual; typically apatite seen in Zambian emerald is smaller, like the crystal near the bottom of this image, which is about 0.15 mm. Photomicrograph by H. Zwaan; magnified 80×.

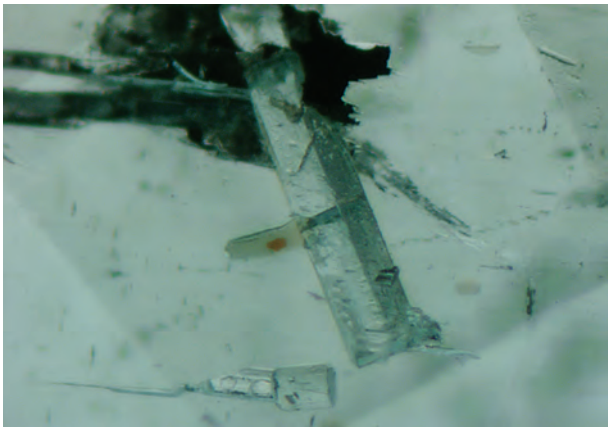

vibrations at 442 and 616 cm^{-1}, and a qualitative EDXRF micro-analysis confirmed the abundance of Ti, with lesser amounts of Nb and Fe, and some Ta.

Growth Features. Widespread in the Chantete emeralds were parallel growth lines with a fine lamellar appearance (again, see figure 32). When observed between crossed polarizers, two samples showed strain that was oriented parallel to the growth lines; none of the other samples showed evidence of strain. In many of the samples, the color was evenly distributed. Others exhibited moderate to strong narrow zoning of straight, alternating light green to medium-dark green bands (figure 36), which was oriented parallel to the prism faces of the crystals (figure 37). When this color zoning was present in faceted stones, it was often well disguised by cutting the table of the emerald parallel to one of the prismatic faces, so that the color zoning could be observed only when looking at the stone from the side, through the pavilion. In some cuttable rough samples, hexagonal color zoning was prominent, often showing a darker green rim and a lighter or darker green core, with alternating lighter and darker green zones in between.

Figure 31. This backscattered electron image shows a minute euhedral inclusion that was identified as fluorapatite by electron-microprobe analysis at the surface of a heavily included emerald. The fluorapatite itself contains small laths of actinolite (darker gray) and magnetite (white). Micrograph by W. J. Lustenhouwer.

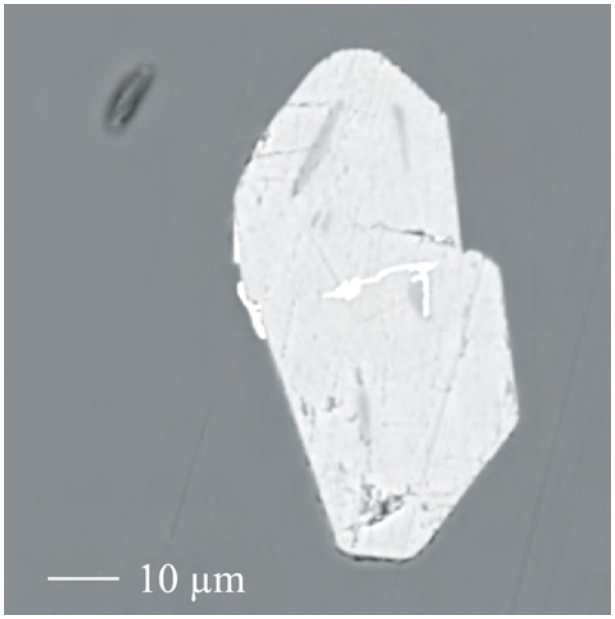

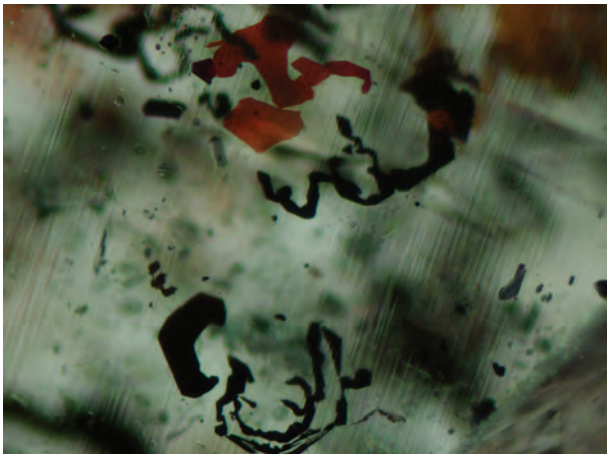

Figure 32. Magnetite in Kafubu emeralds occurs as tiny opaque inclusions, sometimes in parallel planes and showing skeletal shapes. The red-brown inclusions are hematite. Note also the fine-scale parallel growth lines traversing the image. Photomicrograph by H. Zwaan; magnified 65×.

CHEMICAL COMPOSITION

Representative electron-microprobe analyses of emeralds from the Chantete mine and Kagem mining area are shown in table 2 (see *G&G* Data Depository for all analyses). In total, we obtained 78 microprobe analyses of 15 Chantete samples, and 36 analyses of 12 Kagem emeralds. Data from both mining areas were quite similar, although slightly higher

Figure 33. A few of the faceted Zambian emeralds contained large, open-ended, sharp-edged columnar cavities that have the appearance of dissolved actinolite inclusions. These cavities were partially filled with epigenetic debris. Photomicrograph by H. Zwaan; magnified 65×.

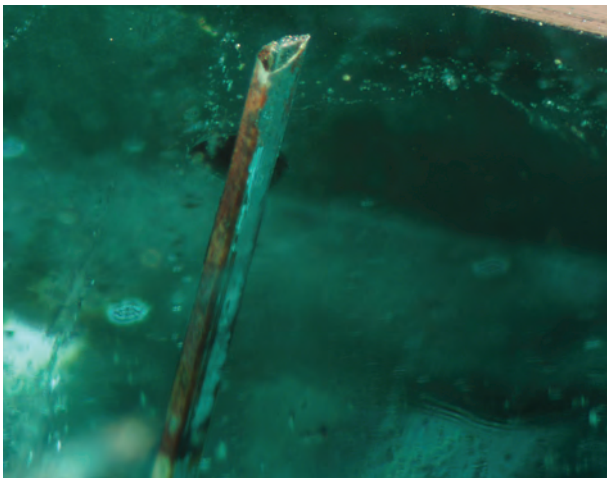

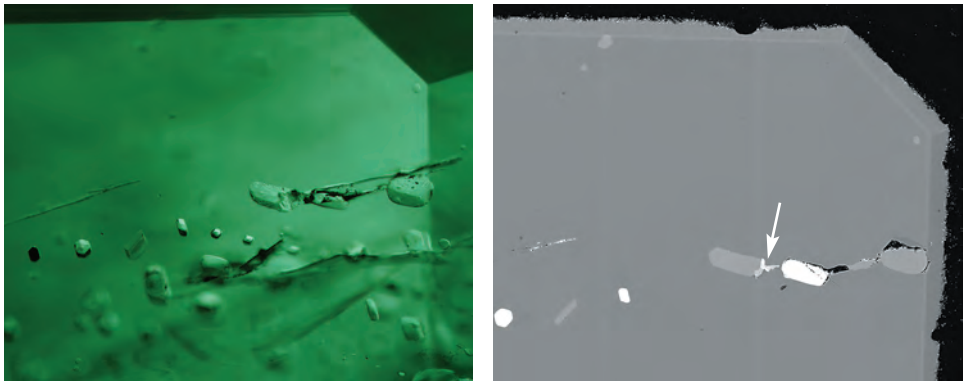

Figure 34. Inclusions showing low and higher relief (left) were identified as quartz and fluorite, respectively. (Photomicrograph by H. Zwaan; magnified 100×.) In the backscattered electron image on the right, the fluorite crystals appear white, while the quartz grains look gray. Carbonates (light gray, see arrow) also were present. Micrograph by W. J. Lustenhouwer; width of view 1.0 mm.

Cr and Fe concentrations were measured in the Kagem stones overall. In addition, the Kagem emeralds showed larger overall variations in the concentration of these elements, as well as in Mg and Na.

The Kagem emeralds were carefully selected to include the lightest to darkest colors seen in commercially available cut stones (see, e.g., figure 15). The color range of the faceted Chantete emeralds tested was more restricted to a typically desirable medium bluish green (see, e.g., figure 16), although considerable color variations were present in one of the rough gem-quality samples of Chantete emerald (again, see figure 37). The most important chromophore in Zambian emeralds is Cr, which averaged 0.26 wt.%—and ranged up to 0.84 wt.%—Cr_2O_3. Overall, the darkest green stones had significantly higher Cr contents than the lighter and medium green stones, which often showed no straightforward correlation between color intensity and average Cr content. In contrast, V concentrations were consistently low, averaging just 0.02 wt.% V_2O_3 and attaining a maximum of 0.09 wt.% V_2O_3. The only other significant chromophoric element was Fe, which averaged 0.76 wt.% oxide (as FeO) and showed a maximum of 1.75 wt.% FeO.

The emeralds contained relatively high concentrations of Mg (average of 1.90 wt.% MgO) and somewhat less Na (average of 1.10 wt.% Na_2O). We detected trace amounts of Ca and K in many of the samples. In the 12 Chantete emeralds analyzed at the University of New Orleans, Ti and Mn were near or below the detection limits in all stones. In the 15 emeralds analyzed at the Free University of Amsterdam, traces of Cs were detected in most samples, Sc was documented in some of them, and Rb was below the detection limit in all the analyses.

Distinct compositional variations were recorded in analyses of fine-scale color zones in a rough emerald from the Chantete mine (again, see figures 37

Figure 35. Reddish orange inclusions of niobian rutile were identified in a thin section of an emerald from the Mbuwa mine. Photomicrograph by H. Zwaan; width of view 1.8 mm.

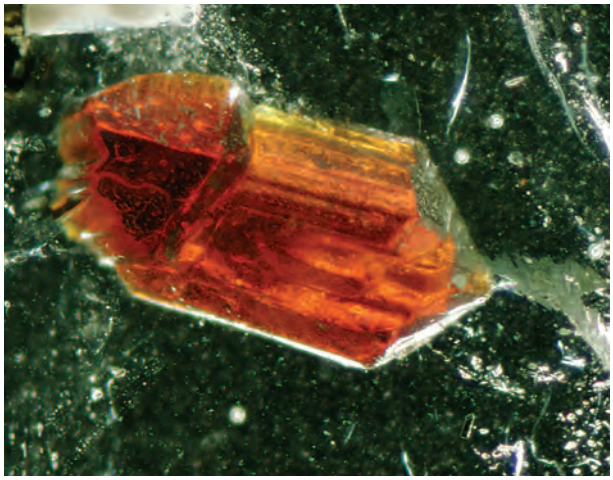

Figure 36. Although an even color appearance is very common in Zambian emeralds, straight narrow color zoning, as in this heavily included 5.69 ct cabochon, was also seen in certain orientations. Photomicrograph by H. Zwaan.

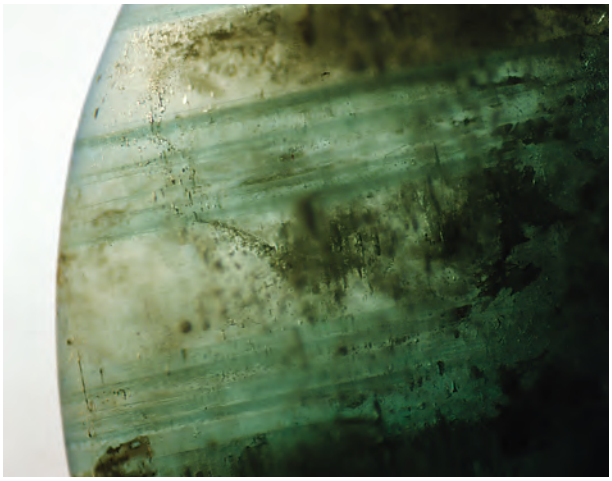

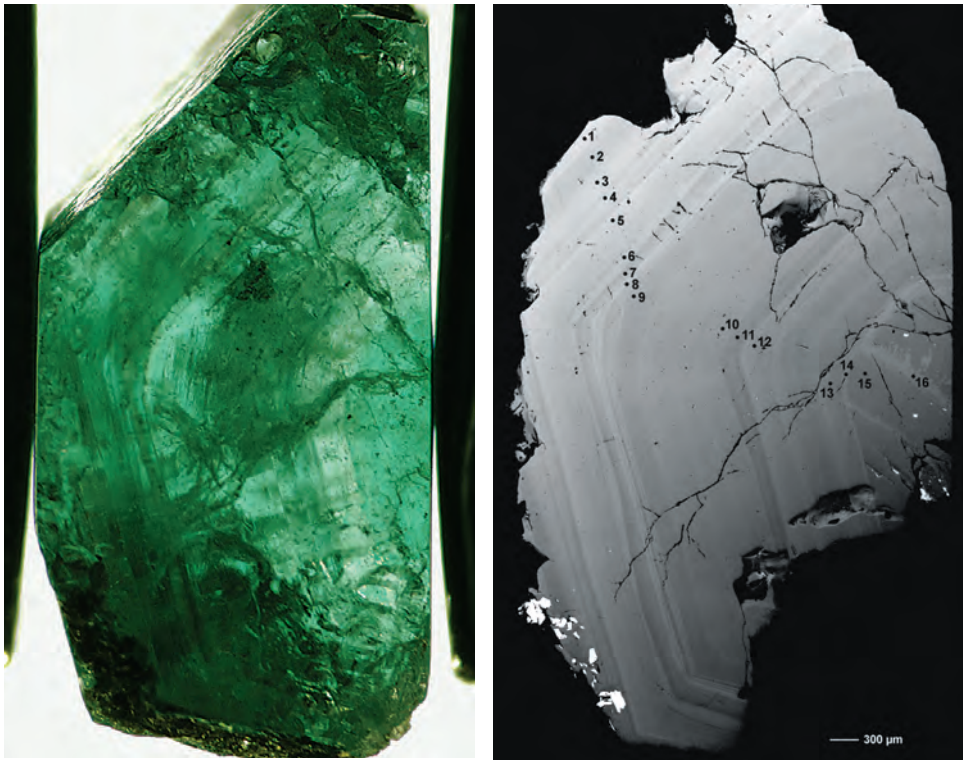

Figure 37. On the left, hexagonal color zoning was observed parallel to the prismatic crystal faces in this 4.93 ct cuttable emerald crystal from the Chantete mine (no. r29, table 2). (Photomicrograph by H. Zwaan; magnified 10×). The backscattered electron image of this same crystal, on the right, also reveals fine-scale growth zoning as well as the position of the spots that were analyzed by electron microprobe. The white-appearing grains are phlogopite. Composite micrograph by W. J. Lustenhouwer.

and 38). The Cr_2O_3 for this emerald ranged from not detectable in a narrow colorless zone to 0.46 wt.% in the darkest green zone, with an average of 0.22 wt.%. As shown in figure 38, there was a good correlation between color and Cr content. Compared to Cr, similar trends were shown by Fe, Mg, and Na, and an inverse pattern was found for Al. The Cs content, which ranged from 0.05 to 0.23 wt.% Cs_2O, was highest in the outer portion of the crystal.

In addition to the elements detected by electron microprobe, EDXRF analysis of the faceted Chantete emeralds found traces of Ga and Zn in separate emeralds, with Ga possibly present in an additional sample. This technique, which is more sensitive than the electron microprobe, detected Mg, K, Ca, Cr, Fe, Rb, and Cs in all 12 of the samples analyzed. V also was detected in five samples, and possibly in two others.

SPECTROSCOPY

Typical UV-Vis-NIR absorption spectra for Zambian emeralds are illustrated in figure 39. The ordinary ray ($E \perp c$) showed bands at 372, 440, 478, 610, 637, and 830, as well as a doublet at 680 and 683 nm. The bands at 440, 610, and 830 nm are broad and the positions were estimated. The extraordinary ray ($E \parallel c$) displayed bands at 425 and 650 nm, as well as absorptions at 632, 662, 684, and 830 nm. Though the intensities varied, all the samples showed the same bands for both the ordinary and extraordinary rays. The bands at 440 and 610, and at 425 and 650 nm, and the peak at 684 nm, indicate the presence of Cr^{3+}, which causes the green color (Wood and Nassau, 1968; Schmetzer et al., 1974). Additional weaker peaks at 478, 662, 684, and the doublet at 680 and 683 nm also are caused by the presence of Cr^{3+}. The shift in absorption from 440 to 425 nm and from 610 to 650 nm causes an absorption minimum at about 512 nm for the ordinary ray, producing a yellowish green color, and a shift toward a minimum at about 500 nm for the extraordinary ray, producing a bluish green color. The band at 830 nm indicates the presence of Fe^{2+} (Platonov et al., 1978), whereas the peak at 372 nm denotes the presence of Fe^{3+} (Schmetzer et al., 1974). The exact Fe^{2+}/Fe^{3+} ratio cannot be determined by this method.

The FTIR spectra of the emeralds contained the typical features caused by vibration of H_2O molecules (see, e.g., figure 40). The most obvious peaks, at 7096 and 5265 cm^{-1}, are caused by type II H_2O molecules, which are present in the channels of the crystal structure of beryl. These water molecules are located adjacent to alkali-metal ions in the channels (Wood and Nassau, 1968), which in the Zambian emeralds are mainly Na^+, Cs^+, and Li^+. The H-H direction of the type II H_2O molecules is

TABLE 2. Representative chemical compositions of Zambian emeralds by electron microprobe.[a]

	Chantete mine						Kagem mining area						
Sample	0.95-2	0.66-2	3.47-2	r29-7	r29-12	r29-5	z01r-1	z08b	z08d	z04c	z03c	z09c	z43a
Weight (ct)	0.95	0.66	3.47	4.93	4.93	4.93	0.55	0.91	0.91	0.66	1.04	0.89	0.98
Color[b]	Med. bG	Med. bG	Med. bG	Color-less	Med. bG	Int. med. bG	Lt. bG	Med. sl. bG	Med. sl. bG	Med. bG	Med. bG	Int. med. sl. bG	Dark bG
Laboratory	UNO[c]	UNO	UNO	FUA[d]	FUA	FUA	FUA	FUA	FUA	FUA	FUA	FUA	FUA
Oxides (wt.%)													
SiO_2	65.39	65.24	64.86	63.52	63.21	62.29	63.40	62.44	62.14	63.17	63.08	62.71	63.35
TiO_2	bdl	bdl	bdl	na	na	na	na	na	na	na	na	na	na
Al_2O_3	15.42	15.33	14.81	15.81	14.97	13.58	15.96	13.65	13.62	14.09	14.39	13.63	14.62
Cr_2O_3	0.08	0.20	0.63	bdl	0.25	0.46	0.25	0.04	0.29	0.15	0.31	0.33	0.70
V_2O_3	0.01	0.04	0.02	0.04	0.02	0.04	0.06	0.02	0.02	0.02	0.02	0.03	0.03
Sc_2O_3	na	na	na	bdl	0.01	0.03	0.03	bdl	bdl	bdl	bdl	bdl	bdl
BeO (calc.)	13.61	13.57	13.52	13.20	13.10	12.89	13.21	12.93	12.88	13.12	13.08	12.99	13.19
FeO^{tot}	0.37	0.34	0.90	0.58	0.72	1.31	0.36	1.11	1.05	1.10	0.96	0.93	1.01
MnO	bdl	bdl	0.01	na	na	na	na	na	na	na	na	na	na
MgO	2.39	2.22	2.47	1.48	1.84	2.36	1.26	2.77	2.68	2.45	2.11	2.90	1.81
CaO	bdl	bdl	bdl	0.02	0.02	0.02	0.03	0.03	0.06	0.06	0.05	0.07	0.04
Na_2O	1.46	1.71	1.36	0.76	0.74	0.98	1.04	0.99	0.94	1.49	1.15	0.86	1.45
K_2O	bdl	bdl	bdl	0.02	0.03	0.04	0.02	0.26	0.25	0.05	0.04	0.21	0.03
Rb_2O	na	na	na	bdl	bdl	bdl	bdl	bdl	bdl	bdl	bdl	bdl	bdl
Cs_2O	na	na	na	0.23	0.06	0.20	0.04	bdl	0.05	0.08	0.11	0.04	0.15
Total[e]	98.72	98.65	98.59	95.65	94.98	94.20	95.64	94.24	93.97	95.78	95.30	94.71	96.39
Ions based on 18 oxygens													
Si	6.001	6.000	5.990	6.010	6.026	6.035	5.996	6.031	6.024	6.013	6.021	6.027	5.997
Ti	bdl	bdl	bdl	na	na	na	na	na	na	na	na	na	na
Al	1.668	1.662	1.612	1.763	1.682	1.551	1.779	1.554	1.556	1.581	1.619	1.544	1.631
Cr	0.006	0.014	0.046	bdl	0.019	0.035	0.019	0.003	0.023	0.011	0.023	0.025	0.053
V	0.001	0.003	0.001	0.003	0.002	0.003	0.004	0.001	0.001	0.002	0.002	0.002	0.003
Sc	na	na	na	bdl	0.001	0.003	0.002	bdl	bdl	bdl	bdl	bdl	bdl
Be	3.001	2.999	3.000	3.000	3.000	3.000	3.000	3.000	3.000	3.000	3.000	3.000	3.000
Fe	0.028	0.026	0.070	0.046	0.057	0.106	0.028	0.090	0.085	0.087	0.076	0.075	0.080
Mn	bdl	bdl	0.001	na	na	na	na	na	na	na	na	na	na
Mg	0.327	0.304	0.340	0.208	0.262	0.340	0.178	0.398	0.387	0.347	0.300	0.415	0.256
Ca	bdl	bdl	bdl	0.002	0.002	0.002	0.003	0.003	0.006	0.006	0.005	0.007	0.004
Na	0.260	0.305	0.244	0.139	0.137	0.185	0.190	0.186	0.176	0.276	0.212	0.160	0.265
K	bdl	bdl	bdl	0.002	0.004	0.005	0.002	0.032	0.031	0.006	0.005	0.026	0.003
Rb	na	na	na	bdl	bdl	bdl	bdl	bdl	bdl	bdl	bdl	bdl	bdl
Cs	na	na	na	0.009	0.002	0.008	0.002	bdl	0.002	0.003	0.005	0.001	0.006

[a] *BeO was calculated based on an assumed stoichiometry of 3 Be atoms per formula unit. Abbreviations: bdl = below detection limit, bG = bluish green, Int. = intense, Lt. = light, med. = medium, na = not analyzed, and sl = slightly.*

[b] *Refers to overall color appearance, except for sample r29, in which specific color zones that correspond to each analysis are listed for this gem-quality crystal (which had an overall color appearance of medium slightly bluish green). The relatively low values for Cr measured in some stones does not appear to correlate with their bluish green color. Since the electron microprobe is a microbeam technique, the particular points analyzed on each of those stones may not be representative of the bulk composition of those samples, particularly if color zoning is present.*

[c] *Analyses performed at the University of New Orleans, Louisiana. Background counts were determined by a mean atomic number (MAN) method (Donovan and Tingle, 1996). Analytical standards included both natural and synthetic materials: albite (Na), adularia (K), quartz and clinopyroxene (Mg, Ca, Fe, and Ti), chromite (Cr), rhodonite (Mn), V_2O_5 (V), PbO (Pb), ZnO (Zn), Bi-germanate (Bi), and sillimanite (Si and Al). MAN standards in addition to the above as appropriate: MgO, hematite, rutile, strontium sulfate, and ZrO_2. Detection limits (in wt.%): TiO_2 = 0.009, CaO = 0.008, MnO = 0.005, and K_2O = 0.012. Cl was analyzed but not detected.*

[d] *Analyses performed at the Free University of Amsterdam, the Netherlands. Analytical standards included both natural and synthetic materials: diopside (Si, Mg, and Ca), corundum (Al), fayalite (Fe), Sc_2O_3 (Sc), jadeite (Na), orthoclase (K), V_2O_5 (V), Cr_2O_3 (Cr), RbBr (Rb), Cs_2ReCl_6 (Cs), fluorite (F), and marialite (Cl). Detection limits (in wt.%): Cr_2O_3 = 0.018, Sc_2O_3 = 0.012, Cs_2O = 0.028, and Rb_2O = 0.029. Cl was analyzed but not detected. Low overall totals appear mainly due to low analytical SiO_2 data.*

[e] *Analyses do not include H_2O. Data on Kafubu emeralds from Hickman (1972) and Banerjee (1995) showed 2.5 wt.% H_2O, and 2.61 and 2.69 wt.% H_2O, respectively.*

Figure 38. Electron-microprobe analyses of the Chantete emerald in figure 37 revealed systematic variations in the composition of the various growth zones. There was a good correlation between color and Cr content, with similar trends shown by Fe, Mg, and Na; the trends for all these elements were opposite that of Al. A significant increase in Cs was evident in the outer portion of the crystal.

perpendicular to the c-axis; the intensity of these peaks was very strong in all the spectra we obtained. Wood and Nassau (1967) demonstrated that their intensity increases as the amount of alkalis increases. The broad band between roughly 3900 and 3400 cm^{-1} is caused by type I and type II H_2O molecules. Type I H_2O molecules are freely present in the channels, without being linked to other ions, and their H-H direction is parallel to the c-axis of the beryl crystal. The peak at 2357 cm^{-1} is caused by CO_2. This peak was present in all the samples for which spectra were taken, but the intensity varied between samples. Similar UV-Vis-NIR and FTIR spectra were described by Milisenda et al. (1999), and UV-Vis spectra of a light green emerald from the Miku mine were illustrated by Schmetzer and Bank (1981).

FTIR spectroscopy also is helpful to identify possible fillers used for clarity enhancement (see e.g., Johnson et al., 1999; Kiefert et al., 1999). None of the spectra we obtained indicated the presence of an artificial resin in any of the stones examined. Also, we did not observe any yellow or blue flash effects (a possible indication that an artificial resin might be present) in the fissures, except for an apparent local blue flash effect observed in one stone from the Chantete

Figure 39. These polarized absorption spectra of an emerald from the Chantete mine show bands that are representative of all the Kafubu samples, and indicate the presence of not only Cr^{3+} and Fe^{2+}, but also Fe^{3+}. The intensities of the bands varied somewhat between samples, but no straightforward relationship could be established between band intensities and Cr and Fe concentrations (or FeO/Cr_2O_3 ratios) measured by electron microprobe. The spectra shown here were collected on a 4.27 ct emerald cut that contained an average of 0.17 wt.% Cr_2O_3 and 0.36 wt.% FeO^{tot}.

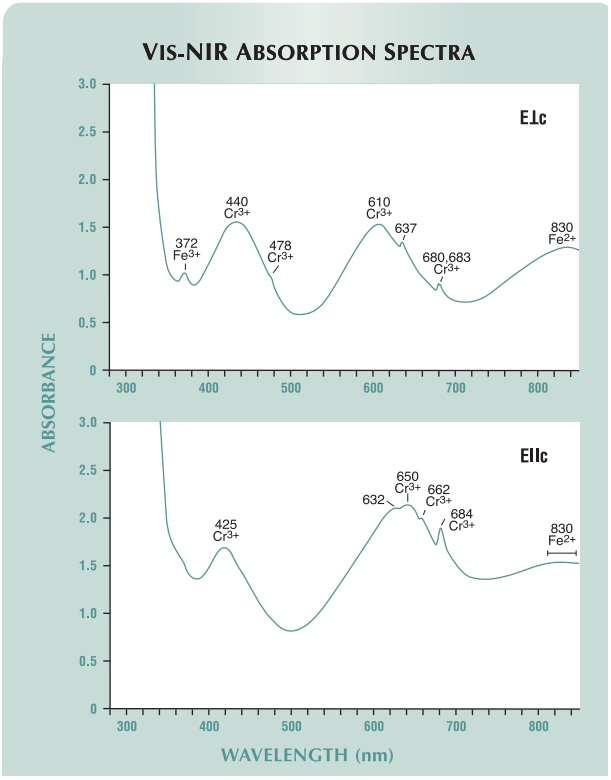

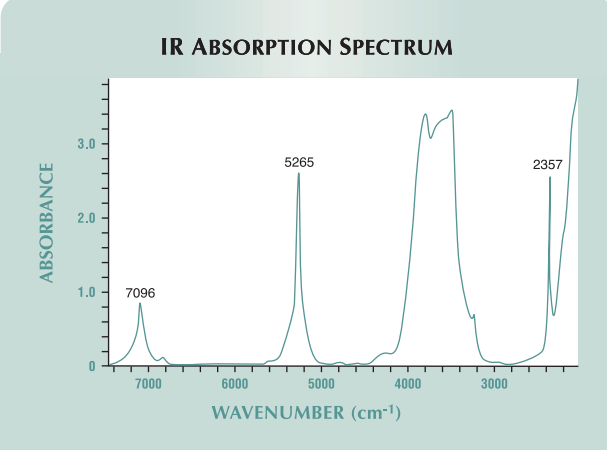

Figure 40. This representative FTIR spectrum of a Kafubu emerald shows peaks at 7096 and 5265 cm^{-1} that are caused by the vibrations of water molecules adjacent to alkali-metal ions in the channels of the beryl structure. The broad band between 3900 and 3400 cm^{-1} also is caused by water molecules in this position, and by free water molecules. The peak at 2357 cm^{-1} is due to CO_2. The intensity of this peak varied substantially between samples.

Figure 41. Peaks in the 3100–2800 cm^{-1} range were seen in the FTIR spectra of both faceted and cuttable rough specimens of Kafubu emerald, indicating the presence of oil. No artificial resin was found in the stones that were tested. Spectra have been offset vertically for clarity.

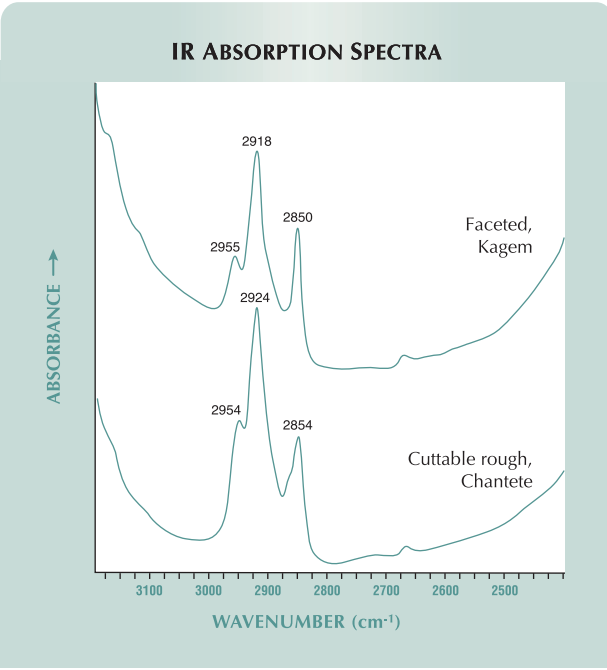

mine, as described in the Microscopic Characteristics section. Stones with sufficient fractures containing a near-colorless filler showed FTIR spectra that are typical for an oil (figure 41). Although the type of oil cannot be established with this method, at the Chantete mine we were told that Johnson's baby oil (mineral oil) is used on the rough. Likewise, mineral oil is reportedly used by emerald cutters in Israel. No green fillers were seen in any of the samples.

DISCUSSION

Physical Properties. The measured refractive indices and specific gravity values (table 1) are fairly consistent with those presented by Milisenda et al. (1999). An unusual dark bluish green emerald described by Schmetzer and Bank (1981) showed extreme values for refractive indices, n_o = 1.602 and n_e = 1.592, with a birefringence of 0.010.

Inclusions in Zambian emeralds have been described by Campbell (1973), Koivula (1982, 1984), Graziani et al. (1984), Gübelin and Koivula (1986), Milisenda et al. (1999), and Moroz and Eliezri (1999). These studies largely agree with and support our findings (table 1). However, in the present study, we did not encounter glauconite, chrysoberyl, margarite, muscovite, or chrysotile, which suggests these mineral inclusions are rare. It should also be noted that the chrysoberyl, margarite, and muscovite were identified in a heavily included crystal fragment (Graziani et al., 1983), which may not be representative of gem-quality material. The presence of isolated CO_2-CH_4–bearing negative crystals has not been reported previously in Zambian emerald.

Chemical Properties. Our chemical analyses showed a wider range of trace-element concentrations than was indicated by the seven analyses presented by Milisenda et al. (1999). Our Cr content was fairly consistent with their results but was slightly higher in some stones; V, Fe, Mg, Ca, Na, and K also showed a much wider range. In addition, our study indicated the presence of Cs and occasionally Sc. The values we measured for the main trace elements all fell within the ranges that were presented earlier by Graziani et al. (1984) on one emerald, Hänni (1982) on two emeralds, Schwarz and Henn (1992) on 11 emeralds from the Kamakanga mine (mean concentrations only), and Moroz et al. (1998) and Moroz and Eliezri (1998) on three samples. Our data also were consistent with the

analyses of noncuttable rough Zambian emeralds reported by Seifert et al. (2004c), except those rough samples had slightly higher Na. Moreover, we found a wider range of Mg and Fe concentrations, with lower values in light green cut emeralds.

Using Schwarz's empirical subdivision of low, medium, and high concentrations of elements in emerald (see, e.g., Schwarz, 1990a,b; Schwarz and Henn, 1992), the Zambian stones generally show a low V content, a moderate amount of Cr, Mg, and Na, and a moderate-to-high Fe content. Notable is the relatively high Cs content in many of our samples. As observed by Bakakin and Belov (1962), Cs is typically present in Li-rich beryl. Li could not be analyzed by electron microprobe, but PIXE/PIGE analyses of 11 Zambian crystal fragments by Calligaro et al. (2000) indicated an average Li content of 580 ppm, along with a high average Cs content of 1,150 ppm.

Examination of the growth zoning in the Chantete emerald crystal (figure 38) showed that as Cr, Fe, and Mg increase, Al decreases. This is expected from the known substitutions in emerald (Aurisicchio et al., 1988), namely of Al^{3+} in the octahedral site by Fe^{2+} and Mg^{2+}, plus Fe^{3+}, Cr^{3+}, and V^{3+}. The presence of Cs^{+}, which is located in the channel of the beryl structure, is coupled with the substitution of Li^{+} for Be^{2+} in the tetrahedral site and clearly follows a different trend. Na appears to reflect mainly the trend of Cr, Fe, and Mg, but also seems to follow the general trend of Cs. This could be explained by the fact that Na^{+} can be involved in coupled substitutions for Al^{3+} in the octahedral site, but also for Be^{2+} in the tetrahedral site (compare, e.g., to Aurisicchio et al., 1988; Barton and Young, 2002). From the trend shown in figure 38, it is clear that the main substitution in the Chantete emerald crystal took place in the Al^{3+} octahedral site.

The analyses of the faceted emeralds did not show a consistent correlation between color and Cr content (see table 2 and the *G&G* Data Depository). However, analysis of the various color zones in the Chantete emerald described above provided a good opportunity to explore the relationship between color and trace-element content within a single crystal. When the data from this crystal are graphed according to the atomic ratios that were plotted by Barton and Young (2002), a clear trend is revealed that confirms Cr as the main chromophore (figure 42). Also plotted in figure 42 are two of the darkest green emeralds analyzed for this study (from Kagem), which extend the trend shown by the zoned Chantete sample. This trend resembles the one diagramed by

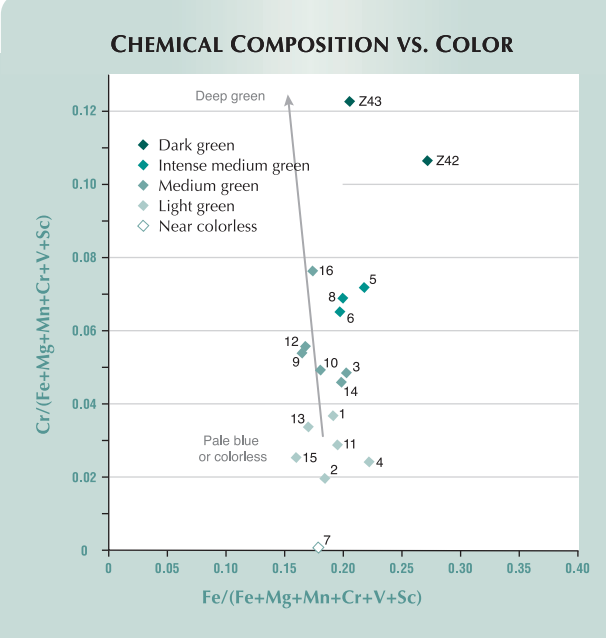

Figure 42. Data from the color-zoned Chantete emerald crystal in figures 37 and 38, together with two of the darkest green emeralds analyzed for this study, are plotted on this beryl composition diagram from Barton and Young (2002) to reveal the relationship between composition and color. The data points are labeled according to the growth zones shown in figure 37, and plotted by color. A clear correlation is revealed between the depth of emerald coloration and Cr content. The arrow (from Barton and Young, 2002) indicates the general trend of beryls from Somondoco (Colombia) and Khaltaro (Pakistan) that range from colorless or pale blue to deep green.

Barton and Young (2002) for pale blue to dark green beryls from Somondoco, Colombia and Khaltaro, Pakistan. The non-emerald analyses from those localities contained very little or no Cr and plotted along the X-axis, like the colorless zone (analysis no. 7) of the Chantete emerald in this study.

Identification. *Separation from Synthetics.* The higher R.I. values of Zambian emeralds (table 1) make them easy to distinguish from their synthetic counterparts. Synthetic emeralds typically have lower refractive indices—roughly between 1.56 and 1.58—and lower specific gravities of 2.65–2.70 (see, e.g., Schrader, 1983; Liddicoat, 1989; Webster, 1994; Schmetzer et al., 1997), although some Russian hydrothermal synthetic emeralds have shown R.I.'s up to 1.584 and S.G.'s up to 2.73 (Webster, 1994;

Koivula et al., 1996). Russian hydrothermal synthetic emeralds can be readily separated from natural emeralds by their distinctive chevron growth zoning or, if present, by unusual internal characteristics such as tiny red-brown particles. Only in the absence of these features would infrared or EDXRF spectroscopy be needed to identify this synthetic (Koivula et al., 1996).

Separation from Emeralds of Different Geographic Origin. The commercially important Colombian emeralds typically show lower refractive indices of 1.569–1.580 (e.g., Ringsrud, 1986; Gübelin, 1989; Boehm, 2002), although Bosshart (1991) gave a wider R.I. range of 1.565–1.588. Colombian emeralds can be further distinguished by their distinctive inclusion scenery, including abundant three-phase inclusions containing halite cubes.

A comparison of other commercially available emeralds with R.I., birefringence, and S.G. values similar to those from Kafubu is shown in table 3 and discussed below. As previously mentioned, roughly 70% of the Zambian stones tested showed n_o = 1.591–1.595 and n_e = 1.583–1.587. Only some light green stones had R.I. values below 1.583, and dark green stones may show R.I.'s above 1.595. According to these data, accurate measurement of the R.I. can distinguish most of the commercial medium and dark green Zambian emeralds from the emeralds of Itabira, Brazil. In addition, the R.I.'s of most Zambian emeralds appear to show only a slight overlap with those of emeralds from the Ural Mountains.

The internal features seen in emeralds from the various localities in table 3 show many similarities, so their use for determining geographic origin is rather limited (for further discussion, see Schwarz, 1998). This overlap is due to the similar geologic environment in which these emeralds form (various types of metamorphic schist). Nevertheless, some distinguishing internal features are listed in table 3. When present, these characteristics can be used to clearly separate Kafubu emeralds from those of Santa Terezinha de Goiás (Brazil), Sandawana (Zimbabwe), and the Swat Valley (Pakistan).

The UV-Vis spectra can only help distinguish between the various emerald occurrences to a limited extent, by indicating differences in the valence state of iron. Only the UV-Vis spectra of Sandawana and, possibly, Ural emeralds show distinctive features. Interestingly, this method can also be used effectively to distinguish between emeralds from Nigeria (containing Fe^{2+} and Fe^{3+}) and Colombia (virtually no iron and no Fe^{3+}; Henn and Bank, 1991; Moroz et al., 1999), which may contain very similar three-phase inclusions. Note that Nigerian emeralds also fall outside the scope of our discussion due to their lower optical properties.

The chemical composition of the various emeralds in table 3 shows considerable overlap. However, trace elements may help eliminate some localities for a specific stone. For instance, relatively high K contents have been documented in emeralds from Kafubu and Mananjary.

PIXE/PIGE analysis, which is a highly sensitive technique that is capable of measuring light elements such as Li, has revealed interesting trends for Cs, Li, and Rb (Calligaro et al., 2000; table 3). Compared to Kafubu, emeralds from Mananjary showed lower Li content, and those from Habachtal had smaller amounts of Rb. Enriched Cs is indicative of emeralds from Kafubu, Mananjary, and Sandawana. The validity of these trends should be tested further with additional analyses of representative samples from the various deposits.

Measuring stable oxygen isotope ratios is another (not entirely nondestructive) technique that can provide additional information. This technique was first applied to Zambian emeralds by Eliezri and Kolodny (1997), and has seen wider application to emeralds from various deposits by Giuliani et al. (1998, 2000). The oxygen isotope data are expressed as $\delta^{18}O$, which is the relative difference between the $^{18}O/^{16}O$ ratio of the sample and that of SMOW (standard mean ocean water), expressed in per mil (‰). The $\delta^{18}O$ values of emeralds from some of the localities in table 3 show considerable overlap (figure 43). Data for Kafubu emeralds exhibit a range similar to that reported for emeralds from the Ural Mountains.

This brief overview shows that even when optical properties, internal characteristics, and chemical data are carefully combined and evaluated, it may not always be possible to differentiate Kafubu emeralds from those of other localities. It appears, however, that in many cases the use of chemical analysis is helpful. Even so, more analyses of representative emeralds from various deposits are needed to better characterize their variations in chemical composition.

SUMMARY AND CONCLUSION

The Kafubu area became a significant producer of good-quality emeralds in the 1970s. As of August 2004, the main production took place at the Kagem, Grizzly, and Chantete concessions, which are all

TABLE 3. Properties of emeralds with R.I. and S.G. values similar to those from Kafubu, Zambia.

Properties	Kafubu area, Zambia	Santa Terezinha de Goiás, Brazil	Itabira district, Brazil	Ural Mountains, Russia	Mananjary region, Madagascar
Physical and optical properties					
References	This study, Milisenda et al. (1999)	Lind et al. (1986), Schwarz (1990a; 2001)	Hänni et al. (1987), Schwarz et al. (1988), Epstein (1989), Henn and Bank (1991); Gübelin (1989), Schwarz (1998), Zwaan (2001)	Gübelin (1974), Sinkankas (1981), Bank (1982), Mumme (1982), Schmetzer et al. (1991), Gübelin and Koivula (1986), Laskovenkov and Zhernakov (1995)	Hänni and Klein (1982), Schwarz and Henn (1992), Schwarz (1994)
R.I.					
n_o	1.585–1.599	1.592–1.600	1.580–1.590	1.581–1.591	1.588–1.591
n_e	1.578–1.591	1.584–1.593	1.574–1.583	1.575–1.584	1.580–1.585
Birefringence	0.006–0.009	0.006–0.010	0.004–0.009	0.007	0.006–0.009
S.G.	2.69–2.78	2.75–2.77	2.72–2.74	2.72–2.75	2.68–2.73
Distinguishing internal features	Skeletal magnetite and hematite (if present)	Abundant opaque inclusions, such as black spinel octahedrons; pale brown to colorless carbonate rhombohedra; fluid inclusions are very small and rare	Numerous parallel growth tubes (with remarkable variation of fluid inclusions)	Irregular color distribution (if present)	Elongate quartz crystals, parallel to the c-axis, often associated with growth tubes; fibrous aggregates of talc (if present); rhombohedral carbonate crystals (rare)
Iron peaks in UV-VIS spectra	Fe^{2+} and Fe^{3+} features	Fe^{2+} and Fe^{3+} features	Fe^{2+} and Fe^{3+} features	Fe^{2+} features only, or Fe^{2+} and Fe^{3+} features	Fe^{2+} and Fe^{3+} features
Electron-microprobe data[a]					
References	This study[b]	Schwarz (1990a)	Schwarz (1990b), Zwaan (2001)	Schmetzer et al. (1991), Schwarz (1991)	Hänni and Klein (1982), Schwarz and Henn (1992)
No. analyses	114	15	71	27	7
Oxide (wt.%)					
SiO_2	61.9–65.4	63.8–66.5	63.3–67.0	64.6–66.9	63.3–65.0
TiO_2	bdl	–	≤ 0.04	≤ 0.05	bdl
Al_2O_3	12.5–17.9	12.2–14.3	13.9–16.9	14.2–18.3	12.8–14.6
Cr_2O_3	bdl–0.84	0.06–1.54	0.06–1.42	0.01–0.50	0.08–0.34
V_2O_3	bdl–0.08	≤ 0.08	≤ 0.07	≤ 0.04	≤ 0.03
FeO^{tot}	0.06–1.75	0.77–1.82	0.41–1.30	0.10–1.16	0.91–1.46
MnO	bdl–0.01	≤ 0.02	≤ 0.08	≤ 0.03	–
MgO	0.27–2.90	2.48–3.09	1.39–2.64	0.29–2.23	1.71–3.00
CaO	bdl–0.12	–	≤ 0.10	≤ 0.03	–
Na_2O	0.16–1.99	1.46–1.73	0.79–1.93	0.61–1.72	1.28–2.16
K_2O	bdl–0.27	≤ 0.03	≤ 0.08	≤ 0.07	0.05–0.21
Cs_2O	bdl	–	bdl	–	–
Rb_2O	bdl–0.23	–	bdl	–	–
Sc_2O_3	bdl–0.07	–	–	–	–
Mo_2O_3	–	–	≤ 0.06	–	–
PIXE/PIGE data[c]					
No. samples	11	8	–	20	12
Trace elements (ppm)					
Li	580 (230)	170 (90)	–	720 (260)	130 (70)
Cs	1150 (540)	350 (300)	–	360 (230)	610 (580)
Rb	140 (60)	15 (2)	–	40 (60)	190 (70)

[a] *Abbreviations: bdl = below detection limit; – = no data.*
[b] *The range of composition reported in the literature for Zambian emeralds falls within the analyses obtained for this study.*
[c] *Data from Calligaro et al. (2000), average elemental content from three point analyses per sample in ppm by weight. Standard deviations are given in parentheses. Detection limits (in ppm) for Rb=2, Li=50, and Cs=100.*

Sandawana, Zimbabwe	Swat Valley, Pakistan	Habachtal, Austria
Gübelin (1958), Zwaan et al. (1997)	Henn (1988), Gübelin (1989)	Gübelin (1956), Morteani and Grundmann (1977), Nwe and Grundmann (1990), Schwarz (1991), Gübelin and Koivula (1986), Grundmann (2001)
1.590–1.594	1.584–1.600	1.582–1.597
1.584–1.587	1.578–1.591	1.574–1.590
0.006–0.007	0.006–0.009	0.005–0.007
2.74–2.77	2.70–2.78	2.70–2.77
Abundant thin needles and curved fibers of amphibole; extremely small fluid inclusions (if present); black grains of chromian ilmenorutile (very rare); phlogopite virtually absent	Many two-and three-phase inclusions (similar to Colombia), but with no rectangular to square shapes; common black chromite and rhombohedral dolomite	Commonly show patchy color distribution; most stones are heavily included and fractured (rarely cuttable and only in small sizes)
Fe^{2+} features only	Fe^{2+} and Fe^{3+} features	Fe^{2+} and Fe^{3+} features
Zwaan et al. (1997)	Henn (1988), Hammarstrom (1989)	Schwarz (1991)
41	176	47
62.6–63.2	62.2–65.8	64.6–66.1
≤ 0.05	≤ 0.02	≤ 0.03
13.0–13.7	13.1–15.0	13.3–14.5
0.61–1.33	0.15–2.05	0.01–0.44
0.04–0.07	0.01–0.06	≤ 0.04
0.45–0.82	0.20–2.51	0.61–1.87
bdl	bdl	≤ 0.05
2.52–2.75	2.21–3.10	2.33–2.92
–	bdl	0.02–0.04
2.07–2.41	1.08–2.11	1.54–2.24
0.03–0.06	≤ 0.02	0.01–0.10
0.06–0.10	–	–
–	–	–
bdl	≤0.19	–
bdl	–	≤ 0.04
22	4	13
800 (310)	350 (130)	190 (210)
710 (320)	120 (80)	370 (390)
350 (200)	6 (3)	18 (13)

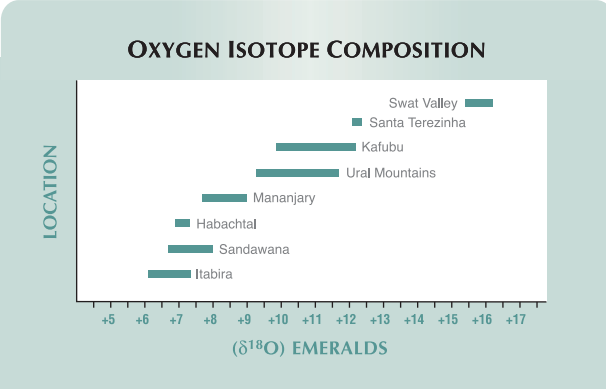

Figure 43. Significant overlap is evident in the oxygen isotopic values of emeralds reported from some of the localities in table 3. The range of $\delta^{18}O$ values for Kafubu emeralds is similar to that for emeralds from the Ural Mountains. Data from Eliezri and Kolodny (1997), Giuliani et al. (1998), Cheilletz et al. (2001), Gavrilenko (2001), and Zwaan et al. (2004).

open-pit mines. Research and exploration activities (e.g., Tembo et al., 2000; Seifert et al., 2004c) demonstrate that the potential for new emerald occurrences in the Kafubu area remains very high.

During a late stage of the Pan-African orogeny, probably around 450 million years ago, emerald mineralization at Kafubu was caused by metasomatic alteration of Cr-bearing metabasites, which were invaded by Be-bearing fluids derived from hydrothermal veins. Economic emerald concentrations are almost entirely confined to phlogopite reaction zones between quartz-tourmaline veins and the metabasites.

Kafubu emeralds show large variations in physical properties, with refractive indices and specific gravities higher than those of emeralds from Colombia, but comparable to emeralds from many other commercially important localities. Kafubu emeralds are characterized by partially healed fractures with various shapes of fluid inclusions. Characteristic mineral inclusions are randomly oriented actinolite needles and phlogopite platelets, and dravite, fluorapatite, magnetite, and hematite. Skeletal magnetite and hematite have not been described as inclusions in emeralds from other occurrences. Inclusions such as dravite, fluorapatite, and fluorite, as well as niobian rutile identified in one stone, confirm a metasomatic origin related to the intrusion of a rare-element pegmatite-hydrothermal vein system.

The chemical composition of the Kafubu emeralds is characterized by a wide range of trace-ele-

ment contents, with generally moderate amounts of Cr, Mg, and Na, and a moderate-to-high iron content as both Fe^{2+} and Fe^{3+}. Notable is a relatively high content of Cs and Li in many samples. The V content is low, and Sc may be detected.

Most of Zambia's emeralds are exported to India, mainly for use in the domestic market, and to Israel for international distribution. Commercial production of emeralds for the international market is done in calibrated sizes; commercial faceted goods typically weigh up to 5 ct, are slightly bluish green to bluish green with medium to dark tones,

Figure 44. Zambia is a recognized source of attractive emeralds that are readily available in calibrated sizes, but occasionally exceptional stones are produced, as shown by the 15.32 ct emerald in this platinum pendant that is set with diamonds. The emerald is unusually large and clean for a Zambian stone, and a laboratory report has verified that it has not been treated in any way. Courtesy of Kothari and Company Inc., Los Angeles, CA; photo © Harold and Erica Van Pelt.

ABOUT THE AUTHORS

Dr. Zwaan is director of the Netherlands Gemmological Laboratory and curator of minerals and gems at the National Museum of Natural History "Naturalis," Leiden, the Netherlands. Drs. Seifert and Vrána are geologists at the Czech Geological Survey, Prague, Czech Republic. Mr. Anckar is a gemologist and geologist with the European Union–funded Mining Sector Diversification Programme (EU-MSDP), Lusaka, Zambia. Mr. Laurs is editor of Gems & Gemology*, and Mr. Muhlmeister is senior research associate in the GIA Gem Laboratory, Carlsbad. Mr. Koivula is chief gemologist at the AGTA Gemological Testing Center laboratory in Carlsbad. Dr. Simmons is professor of mineralogy, and Mr. Falster is analytical instrumentation manager, in the Department of Geology and Geophysics at the University of New Orleans, Louisiana. Mr. Lustenhouwer is chemical analyst in the Faculty of Earth Sciences at the Free University of Amsterdam, the Netherlands. Mr. Garcia-Guillerminet is director of the CCIP French Gemmological Laboratory, Paris, France.*

ACKNOWLEDGMENTS: Chantete Emerald Ltd., Kitwe, Zambia, is thanked for providing valuable information on the mining operation, granting full access to the deposit, and supplying samples for examination. The authors are grateful to Enrico Storti (E&M Storti Mining Ltd., Kitwe, Zambia) for his kind assistance with visiting the Pirala and Twampane mines, and Siradiou Diop (Grizzly Mining Ltd., Kitwe) for accommodating them at the Grizzly mine. Elizabeth P. Quinn, staff gemologist at the GIA Gem Laboratory, Carlsbad, is thanked for providing gemological properties of some emeralds from the Chantete mine. Dr. Andy Hsi-Tien collected the UV-Vis spectra at the GIA Gem Laboratory in Carlsbad.

Avraham Eshed, president of Gemstar Ltd., Ramat Gan, Israel, is thanked for valuable information on mining, production, and distribution; for providing photographs; and for giving access to his cutting factory and the opportunity to inspect a large number of commercial goods that are entering the market. Israel Eliezri (Colgem Ltd., Ramat Gan, Israel) is thanked for loaning samples for examination, and for supplying additional photographs and information. Ashok Sancheti (Pioneer Gems, New York) and Lalit Kothari (Kothari and Company Inc., Los Angeles, California) are thanked for loaning jewelry for photography. Trevor Schultz (Schultz Mining Ltd., Kitwe, Zambia) offered feedback on the run-of-mine production of emerald from the Kafubu area. Govind Gupta (Kagem Mining Ltd., Kitwe, Zambia) gave updated information on the privatization agreement between Hagura and the Government of Zambia. Dharmendra Tank (Heeralal Chhaganlal Tank Manufacturing Jewelers, Jaipur, India) provided information on the international distribution of Zambian emeralds. J. G. Dey, chief geologist at Kagem (Kitwe, Zambia), described the successful drilling operation at the Fwaya-Fwaya Ext. F10 mine. Dirk van der Marel and Jeroen Goud (National Museum of Natural History "Naturalis," Leiden) are thanked for taking photographs, and Dirk also for general assistance.

Facilities for electron-microprobe analyses were provided by the Free University of Amsterdam and by NWO, the Netherlands Organization for Scientific Research. Access to Raman facilities was provided by the CCIP French Gemmological Laboratory, Paris. Electron-microprobe analyses of the samples in box A were performed at Masaryk University in Brno, Czech Republic, by P. Sulovský.

REFERENCES

Aurisicchio C., Fioravanti G., Grubessi O., Zanazzi P.F. (1988) Reappraisal of the crystal chemistry of beryl. *American Mineralogist*, Vol. 73, No. 7–8, pp. 826–837.

Bakakin V.V., Belov N.V. (1962) Crystal chemistry of beryl. *Geokhimiya*, Vol. 5, pp. 420–433.

Banerjee A. (1995) Investigation of fluid inclusion in emeralds of different geological origins by microchemical analysis and IR-reflexion-spectroscopy. *Boletín de la Sociedad Española de Mineralogía*, Vol. 18-1, pp. 18–19.

Bank H. (1982) Geschliffene zonar gebaute Smaragde aus dem Gebiet der Tokowaya, Ural, UdSSR. *Zeitschrift der Deutschen Gemmologischen Gesellschaft*, Vol. 31, No. 3, pp. 193–194.

Barton M.D., Young S. (2002) Non-pegmatitic deposits of beryllium: Mineralogy, geology, phase equilibria and origin. In E.S. Grew, Ed., *Beryllium: Mineralogy, Petrology and Geochemistry*, Reviews in Mineralogy and Geochemistry, Vol. 50, Chapter 14, pp. 591–691.

Boehm E. (2002) Gem News International: New emerald find from the Chivor region, Colombia. *Gems & Gemology*, Vol. 38, No. 4, pp. 350–351.

Bosshart G. (1991) Emeralds from Colombia, part 2. *Journal of Gemmology*, Vol. 22, No. 7, pp. 409–425.

Calligaro T., Dran J.C., Poirot J.P., Querré G., Salomon J., Zwaan J.C. (2000) PIXE/PIGE characterisation of emeralds using an external micro-beam. *Nuclear Instruments and Methods in Physics Research B*, Vol. 161–163, pp. 769–774.

Campbell I.C.C. (1973) Emeralds reputed to be of Zambian origin. *Journal of Gemmology*, Vol. 13, No. 5, pp. 169–179.

Caspi A. (1997) Modern diamond cutting and polishing. *Gems & Gemology*, Vol. 33, No. 2, pp. 102–121.

Cheilletz A., Sabot B., Marchand P., de Donato P., Taylor B., Archibald D., Barrès O., Andrianjaffy J. (2001) Emerald deposits in Madagascar: Two different types for one mineralising event. *EUG XI*, Strasbourg, France, April 8–12, p. 547.

Coats J.S., Mosley P.N., Mankelow J.M., Mwale M., Chikambwe E.M., Muibeya B., Ndhlovu K.C., Nzabara F. (2001) *The Geology and Mineral Resources of Zambia*. Geological Survey Department Memoir 6, Ministry of Mines and Minerals Development, Lusaka, Zambia.

Cook F.A. (1997) Applications of geophysics in gemstone exploration. *Gems & Gemology*, Vol. 33, No. 1, pp. 4–23.

Cosi M., de Bonis A., Gosso G., Hunziker J., Martinotti G., Moratto S., Robert J.P., Ruhlman F. (1992) Late Proterozoic thrust tectonics, high-pressure metamorphism and uranium mineralization in the Domes area, Lufilian Arc, northwestern Zambia. *Precambrian Research*, Vol. 58, No. 1–4, pp. 215–240.

Daly M.C., Unrug R. (1983) The Muva Supergroup of northern Zambia; A craton to mobile belt sedimentary sequence. *Transactions of the Geological Society of South Africa*, Vol. 85, No. 3, pp. 155–165.

de Waele B., Mapani B. (2002) Geology and correlation of the central Irumide belt. *Journal of African Earth Sciences*, Vol. 35, No. 3, pp. 385–397.

de Waele B., Wingate M.T.D., Fitzsimons I.C.W., Mapani B. (2002) Untying the Kibaran knot: A re-assessment of Mesoproterozoic correlations in southern Africa based on SHRIMP U-Pb data from the Irumide belt. *Geology*, Vol. 31, No. 6, pp. 509–512.

Donovan J.J., Tingle T.N. (1996) An improved mean atomic number correction for quantitative microanalysis. *Journal of Microscopy*, Vol. 2, No. 1, pp. 1–7.

Eliezri I.Z., Kolodny Y. (1997) The isotopic composition of oxygen in emeralds as an indicator of origin. *26th International Gemmological Conference*, Idar-Oberstein, Germany, p. 14.

Epstein D.S. (1989) The Capoeirana emerald deposit near Nova Era, Minas Gerais, Brazil. *Gems & Gemology*, Vol. 25, No. 3, pp. 150–158.

Fritsch E., Rondeau B., Notari F., Michelou J.-C., Devouard B., Peucat J.-J., Chalain J.-P., Lulzac Y., de Narvaez D., Arboleda C. (2002) Les nouvelles mines d'émeraude de La Pita (Colombie) 2e partie. *Revue de Gemmologie*, No. 144, 2002, pp. 13–21.

Gavrilenko E. (2001) Emeralds of the Ural mountains (Russia): Geology, fluid inclusions and oxygen isotopes. *28th International Gemmological Conference*, Madrid, Spain, pp. 36–40.

Giuliani G., France-Lanord C., Coget P., Schwarz D., Cheilletz A., Branquet Y., Girard D., Martin-Izard A., Alexandrov P., Piat D.H. (1998) Oxygen isotope systematics of emerald: Relevance for its origin and geological significance. *Mineralium Deposita*, Vol. 33, No. 5, pp. 513–519.

Giuliani G., Chaussidon M., Schubnel H.J., Piat D.H., Rollion-Bard C., France-Lanord C., Giard D., Narvaez D.D., Rondeau B. (2000) Oxygen isotopes and emerald trade routes since antiquity. *Science*, Vol. 287, No. 5453, pp. 631–633.

Graziani G., Gübelin E., Lucchesi S. (1983) The genesis of an emerald from the Kitwe District, Zambia. *Neues Jahrbuch für Mineralogie, Monatshefte*, Vol. 4, pp. 75–186.

Graziani G., Gübelin E., Lucchesi S. (1984) Report on the investigation of an emerald from the Kitwe District, Zambia. *Australian Gemmologist*, Vol. 15, No. 7, pp. 227–234.

Grundmann G. (2001) Die Smaragde der Welt. In D. Schwarz and R. Hochleitner, Eds., *Smaragd—der kostbarste Beryll, der teuerste Edelstein*, extraLapis No. 21, pp. 26–37.

Gübelin E.J. (1958) Emeralds from Sandawana. *Journal of Gemmology*, Vol. 6, No. 8, pp. 340–354.

Gübelin E.J. (1956) The emerald from Habachtal. *Gems & Gemology*, Vol. 8, No. 10, pp. 295–309.

Gübelin E.J. (1974) *Die Innenwelt der Edelsteine*. Hanns Reich Verlag, Düsseldorf, Germany.

Gübelin E.J. (1989) Gemological characteristics of Pakistani emeralds. In A.H. Kazmi and L.W. Snee, Eds., *Emeralds of Pakistan: Geology, Gemology and Genesis*, Van Nostrand Reinhold, New York, pp. 75–92.

Gübelin E., Koivula J.I. (1986) *Photoatlas of Inclusions in Gemstones*. ABC Edition, Zürich, Switzerland.

Hammarstrom J.M. (1989) Mineral chemistry of emeralds and some associated minerals from Pakistan and Afghanistan: An electron microprobe study. In A.H. Kazmi and L.W. Snee, Eds., *Emeralds of Pakistan: Geology, Gemology and Genesis*, Van Nostrand Reinhold, New York, pp. 125–150.

Hänni H. (1982) A contribution to the separability of natural and synthetic emeralds. *Journal of Gemmology*, Vol. 18, No. 2, pp. 138–144.

Hänni H.A., Klein H.H. (1982) Ein Smaragdvorkommen in Madagaskar. *Zeitschrift der Deutschen Gemmologischen Gesellschaft*, Vol. 31, No. 1/2, pp. 71–77.

Hänni H.A., Schwarz D., Fischer M. (1987) The emeralds of the Belmont mine, Minas Gerais, Brazil. *Journal of Gemmology*, Vol. 20, No. 7/8, pp. 446–456.

Henn U. (1988) Untersuchungen an Smaragden aus dem Swat-Tal, Pakistan. *Zeitschrift der Deutschen Gemmologischen Gesellschaft*, Vol. 37, No. 3/4, pp. 121–127.

Henn U., Bank H. (1991) Außergewöhnliche Smaragde aus Nigeria. *Zeitschrift der Deutschen Gemmologischen Gesellschaft*, Vol. 40, No. 4, pp. 181–187.

Hickman A.C.J. (1972) *The Miku Emerald Deposit*. Geological Survey Department Economic Report No. 27, Ministry of Mines and Mining Development, Republic of Zambia, 35 pp.

Hickman A.C.J. (1973) *The Geology of the Luanshya Area*. Report of the Geological Survey No. 46, Ministry of Mines, Republic of Zambia, 32 pp.

John T., Schenk V., Mezger K., Tembo F. (2004) Timing and PT evolution of whiteschist metamorphism in the Lufilian Arc–Zambezi Belt Orogen (Zambia): Implications for the assembly of Gondwana. *Journal of Geology*, Vol. 112, No. 1, pp. 71–90.

Johnson M.L., Elen S., Muhlmeister S. (1999) On the identification of various emerald filling substances. *Gems & Gemology*, Vol. 35, No. 2, pp. 82–107.

Kiefert L., Hänni H.A., Chalain J.-P., Weber W. (1999) Identification of filler substances in emeralds by infrared and Raman spectroscopy. *Journal of Gemmology*, Vol. 26, No. 8, pp. 487–500.

Koivula J.I. (1982) Tourmaline as an inclusion in Zambian emeralds. *Gems & Gemology*, Vol. 18, No. 4, pp. 225–227.

Koivula J.I. (1984) Mineral inclusions in Zambian emeralds. *Australian Gemmologist*, Vol. 15, No. 7, pp. 235–239.

Koivula J.I., Kammerling R.C., DeGhionno D., Reinitz I., Fritsch E., Johnson M.L. (1996) Gemological investigation of a new type of Russian hydrothermal synthetic emerald. *Gems & Gemology*, Vol. 32, No. 1, pp. 32–39.

Kozlowski A., Metz P., Estrada Jaramillo H.A. (1988) Emeralds from Somondoco, Colombia: Chemical composition, fluid inclusions and origin. *Neues Jahrbuch für Mineralogie, Abhandlungen*, Vol. 159, No. 1, pp. 23–49.
Laskovenkov A.F., Zhernakov V.I. (1995) An update on the Ural emerald mines. *Gems & Gemology*, Vol. 31, No. 2, pp. 106–113.
Laurs B. (2004) Gem News International: Update on several gem localities in Zambia and Malawi. *Gems & Gemology*, Vol. 40, No. 4, pp. 347–350.
Leake B.E., Woolley A.R., Arps C.E.S., Birch W.D., Gilbert M.C., Grice J.D., Hawthorne F.C., Kato A., Kisch H.J., Krivovichev V.G., Linthout K., Laird J., Mandarino J., Maresch W.V., Nickel E.H., Rock N.M.S., Schumacher J.C., Smith D.C., Stephenson N.C.N., Ungaretti L., Whittaker E.J.W., Youzhi G. (1997) Nomenclature of amphiboles: Report of the subcommittee on amphiboles of the International Mineralogical Association Commission on New Minerals and Mineral Names. *Mineralogical Magazine*, Vol. 61, No. 2, pp. 295–321.
Liddicoat R.T. (1989) *Handbook of Gem Identification*, 12th ed., 2nd rev. printing. Gemological Institute of America, Santa Monica, CA.
Lind T., Henn U., Bank H. (1986) Smaragde von Sta. Terezinha de Goias, Brasilien, mit relativ hoher Lichtbrechung. *Zeitschrift der Deutschen Gemmologischen Gesellschaft*, Vol. 35, No. 4, pp. 186–187.
Milisenda C.C., Malango V., Taupitz K.C. (1999) Edelsteine aus Sambia—Teil 1: Smaragd. *Zeitschrift der Deutschen Gemmologischen Gesellschaft*, Vol. 48, No. 1, pp. 9–28.
Moroz I., Eliezri I.Z. (1998) Emerald chemistry from different deposits. *Australian Gemmologist*, Vol. 20, No. 2, pp. 64–69.
Moroz I., Eliezri I.Z. (1999) Mineral inclusions in emeralds from different sources. *Journal of Gemmology*, Vol. 26, No. 6, pp. 357–363.
Moroz I., Panczer G., Roth M. (1998) Laser-induced luminescence of emeralds from different sources. *Journal of Gemmology*, Vol. 26, No. 5, pp. 316–320.
Moroz I., Roth M.L., Deich V.B. (1999) The visible absorption spectroscopy of emeralds from different deposits. *Australian Gemmologist*, Vol. 20, No. 8, pp. 315–320.
Morteani G., Grundmann G. (1977) The emerald porphyroblasts in the penninic rocks of the central Tauern Window. *Neues Jahrbuch für Mineralogie, Mitteilungen*, Vol. 11, pp. 509–516.
Mumme I. (1982) *The Emerald*. Mumme Publications, Port Hacking, New South Wales, Australia.
Ng'uni B., Mwamba K. (2004) *Evaluation of the Potential and Authentication of Emerald Mineralization in North-Western Province, Musakashi Area, Chief Mujimanzovu–Solwezi District*. Draft Economic Report, Geological Survey Department, Lusaka, Zambia.
Nwe Y.Y., Grundmann G. (1990) Evolution of metamorphic fluids in shear zones: The record from the emeralds of Habachtal, Tauern Window, Austria. *Lithos*, Vol. 25, No. 4, pp. 281–304.
Parkin J. (2000) *Geology of the St. Francis Mission and Musakashi River Areas. Explanation of Degree Sheet 1226 NE and SE Quarters and Part of 1126 SE Quarter*. Report No. 80, Geological Survey Department, Lusaka, Zambia, 49 pp.
Platonov A.N., Taran M.N., Minko O.E., Polshyn E.V. (1978) Optical absorption spectra and nature of color of iron-containing beryls. *Physics and Chemistry of Minerals*, Vol. 3, No. 1, pp. 87–88.
Ringsrud R. (1986) The Coscuez mine: A major source of Colombian emeralds. *Gems & Gemology*, Vol. 22, No. 2, pp. 67–79.
Samson I., Anderson A., Marshall D. (2003) *Fluid Inclusions, Analysis and Interpretation*. Mineralogical Association of Canada Short Course Series, Vol. 32, 374 pp.
Schmetzer K., Bank H. (1981) An unusual pleochroism in Zambian emeralds. *Journal of Gemmology*, Vol. 17, No. 7, pp. 443–445.
Schmetzer K., Berdesinski W., Bank H. (1974) Über die Mineralart Beryll, ihre Farben und Absorptionsspektren. *Zeitschrift der Deutschen Gemmologischen Gesellschaft*, Vol. 23, No. 1, pp. 5–39.
Schmetzer K., Bernhardt H., Biehler R. (1991) Emeralds from the Ural Mountains, USSR. *Gems & Gemology*, Vol. 27, No. 2, pp. 86–99.
Schmetzer K., Kiefert L., Bernhardt H.-J., Zhang B. (1997) Characterization of Chinese hydrothermal synthetic emerald. *Gems & Gemology*, Vol. 33, No. 4, pp. 276–291.
Schrader H.W. (1983) Contributions to the study of the distinction of natural and synthetic emeralds. *Journal of Gemmology*, Vol. 18, No. 6, pp. 530–543.
Schwarz D. (1990a) Die brasilianischen Smaragde und ihre Vorkommen: Santa Terezinha de Goiás/Go. *Zeitschrift der Deutschen Gemmologischen Gesellschaft*, Vol. 39, No. 1, pp. 13–44.
Schwarz D. (1990b) Die chemische Eigenschaften der Smaragde I. Brasilien. *Zeitschrift der Deutschen Gemmologischen Gesellschaft*, Vol. 39, No. 4, pp. 233–272.
Schwarz D. (1991) Die chemische Eigenschaften der Smaragde III. Habachtal/Österreich und Uralgebirge/UdSSR. *Zeitschrift der Deutschen Gemmologischen Gesellschaft*, Vol. 40, No. 2/3, pp. 103–143.
Schwarz D. (1994) Emeralds from the Mananjary region, Madagascar: Internal features. *Gems & Gemology*, Vol. 30, No. 2, pp. 88–101.
Schwarz D. (1998) The importance of solid and fluid inclusions for the characterization of natural and synthetic emeralds. In D. Giard, Ed., *L'émeraude*, Association Française de Gemmologie, Paris, pp. 71–80.
Schwarz D. (2001) Gemmologie des Smaragds—Ist die Herkunftsbestimmung von Smaragden möglich? In D. Schwarz and R. Hochleitner, Eds., *Smaragd, der kostbarste Beryll, der teuerste Edelstein*, extraLapis No. 21, pp. 68–73.
Schwarz D., Henn U. (1992) Emeralds from Madagascar. *Journal of Gemmology*, Vol. 23, No. 3, pp. 140–149.
Schwarz D., Bank H., Henn U. (1988) Neues Smaragdvorkommen in Brasilien entdeckt: Capoeirana bei Nova Era, Minas Gerais. *Zeitschrift der Deutschen Gemmologischen Gesellschaft*, Vol. 37, No. 3/4, pp. 146–147.
Seifert A.V., Vrána S., Lombe D.K. (2004a) *Evaluation of Mineralization in the Solwezi area, Northwestern Province, Zambia. Final Report for the Year 2004*. Czech Geological Survey, Record Office – File Report No. 2/2004, Prague, Czech Republic, 20 pp.
Seifert A., Vrána S., Lombe D.K., Mwale M. (2004b) *Impact Assessment of Mining of Beryl Mineralization on the Environment in the Kafubu Area; Problems and Solutions*. Final Report for the Year 2003. Czech Geological Survey, Record Office – File Report No. 1/2004, Prague, Czech Republic, 63 pp.
Seifert A.V., Žáček V., Vrána S., Pecina V., Zachariáš J., Zwaan J.C. (2004c) Emerald mineralization in the Kafubu area, Zambia. *Bulletin of Geosciences*, Vol. 79, No. 1, pp. 1–40.
Sinkankas J. (1981) *Emerald and Other Beryls*. Chilton Book Co., Radnor, PA.
Sliwa A.S., Nguluwe C.A. (1984) Geological setting of Zambian emerald deposits. *Precambrian Research*, Vol. 25, pp. 213–228.
Suwa Y. (1994) *Gemstones: Quality and Value*, 8th ed. Gemological Institute of America and Suwa & Son Inc., Santa Monica, CA.
Tembo F., Kambani S., Katongo C., Simasiku S. (2000) *Draft Report on the Geological and Structural Control of Emerald Mineralization in the Ndola Rural Area, Zambia*. University of Zambia, School of Mines, Lusaka, 72 pp.
Viana R.R., Mänttäri I., Kunst H., Jordt-Evangelista H. (2003) Age of pegmatites from eastern Brazil and implications of mica intergrowths on cooling rates and age calculations. *Journal of South American Earth Sciences*, Vol. 16, pp. 493–501.
Webster R. (1994) *Gems: Their Sources, Descriptions and Identification*, 5th ed. Revised by P.G. Read, Butterworth-Heinemann, Oxford, England.
Wood D.L., Nassau K. (1967) Infrared spectra of foreign molecules in beryl. *Journal of Chemical Physics*, Vol. 47, No. 7, pp. 2220–2228.
Wood D.L., Nassau K. (1968) The characterization of beryl and emerald by visible and infrared absorption spectroscopy. *American Mineralogist*, Vol. 53, No. 5–6, pp. 777–799.
Zambia cranks up the emerald sector (2004) *ICA Gazette*, June, pp. 1, 10–11.
Zwaan J.C. (2001) Preliminary study of emeralds from the Piteiras emerald mine, Minas Gerais, Brazil. *28th International Gemmological Conference*, Madrid, Sprain, pp. 106–109.
Zwaan J.C., Kanis J., Petsch E.J. (1997) Update on emeralds from the Sandawana mines, Zimbabwe. *Gems & Gemology*, Vol. 33, No. 2, pp. 80–100.
Zwaan J.C., Cheilletz A., Taylor B.E. (2004) Tracing the emerald origin by oxygen isotope data: The case of Sandawana, Zimbabwe. *Comptes Rendus Geoscience*, Vol. 336, pp. 41–48.